Faculty of Engineering and Technology
Jadavpur University

DEVELOPMENT AND *IN VITRO* CHARACTERIZATION OF APTAMER CONJUGATED DOXORUBICIN LOADED PLGA NANOPARTICLES

Vimal Prakash Mishra
Bachelor of Pharmacy

Thesis submitted in partial fulfillment for the requirements of the degree of
Master of Pharmaceutical Technology, 2016
Examination Roll No: M4PHA1606
Registration No: 129105 of 2014-15

Under the guidance of
Prof. (Dr.) Biswajit Mukherjee
Pharmaceutics Research Laboratory
Department of Pharmaceutical Technology
Jadavpur University, Kolkata-700032, India

Certificate

This is to certify that VIMAL PRAKASH MISHRA (Class Roll: 001411402006, Examination Roll: M4PHA1606 and Reg. No: 129105 of 2014-15) has carried out the research work entitled "DEVELOPMENT AND *IN VITRO* CHARACTERIZATION OF APTAMER CONJUGATED DOXORUBICIN LOADED PLGA NANOPARTICLES" independently with proper care and attention under my supervision and guidance in the Pharmaceutics Research Laboratory in the Department of Pharmaceutical Technology, Jadavpur University. He has incorporated his findings into this thesis of the same title, being submitted by him, in partial fulfillment of the requirements for the degree of **Master of Pharmaceutical Technology** from Jadavpur University. I appreciate his endeavor to do the project and his work has reached my gratification.

.....

Prof. (Dr.) Biswajit Mukherjee
Project supervisor
Department of Pharmaceutical Technology
Jadavpur University
Kolkata, India

.....

Prof. (Dr.) Biswajit Mukherjee
Head of the Department
Department of Pharmaceutical Technology
Jadavpur University
Kolkata, India

.....

Prof. Sivaji Bandyopadhyay
Dean
Faculty of Engineering & Technology
Jadavpur University
Kolkata, India

DECLARATION

I hereby declare that this thesis contains literature survey and original research work by the undersigned candidate, as part of his Master of Pharmaceutical Technology studies. All information in this document have been obtained and presented in accordance with academic rules and ethical conduct.

I also declare that as required by these rules and conduct, I have fully cited and referenced all materials and results that are not original to this work.

NAME	VIMAL PRAKASH MISHRA
EXAMINATION ROLL NUMBER	M4PHA1606
CLASS ROLL NUMBER	001411402006
REGISTRATION NUMBER	129105 of 2014-15
THESIS TITLE	Development & *in vitro* Characterization of aptamer conjugated Doxorubicin loaded PLGA Nanoparticles

VIMAL PRAKASH MISHRA

Acknowledgement

I would like to express my deep gratitude and indebtedness to my project guide **Prof. (Dr.) Biswajit Mukherjee**, Department of Pharmaceutical Technology, Jadavpur University, for his constant assistance and valuable suggestion at every step of my work. His mentorship was paramount in providing a well-rounded experience consistent my long-term career goals. It was his valuable guidance throughout the entire period that has helped me whenever I was in trouble. I convey my special thanks to my seniors of the lab **Samrat Chakraborty, Laboni Mondal, Bhabani Shankar Satapathy** and **Ankan Choudhury** for their valuable support and co-operation which made my work fruitful. I would also like to extend my gratitude to my other seniors of the lab **Niladri Shekhar Dey, Sanchari Bhattacharya, Tapan Shaw, Paramita Paul, Lopamudra Dutta,** my colleagues **Rhitabrita Chakraborty, Ashique Al Hoque** and many others who helped me in various ways during the tenure of my research work. I would also like to acknowledge the **Centre for Research in Nanoscience & Nanotechnology, University of Calcutta, Salt Lake, Kolkata** and **Indian Associations for The Cultivation of Science, Jadavpur, Kolkata** for their assistance in providing me with the facilities of **Scanning Electron Microscopy** and **Field Emmission Scanning Electron Microscopy** respectively for the purpose of my research work. I thank my parents for their faith in me and allowing me to be as ambitious as I wanted. It was under their watchful eye that I gained so much drive and an ability to tackle challenges head on. Last but not the least, I convey my gratitude towards the entire **Department of Pharmaceutical Technology**, the **Faculty of Engineering & Technology** and the academic administration of the **Jadavpur University** for providing me with the opportunity of being a part of this Department and the University and conducting this research work.

Dedicated to my parents

and my guide

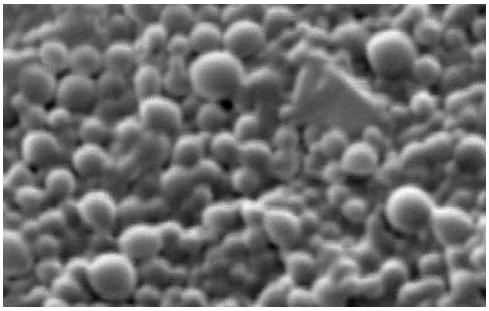

Development & *in vitro* Characterization of aptamer conjugated Doxorubicin loaded PLGA Nanoparticles

Vimal Prakash Mishra

Department of Pharmaceutical Technology
Faculty of Engineering & Technology
Jadavpur University, Kolkata
2016

CONTENTS

Chapter - 1

Nanotechnology: An Overview

NANOTECHNOLOGY: AN OVERVIEW

1.1 Background

Nanoscience involves the study of the control of matter on an atomic and molecular scale. This molecular level investigation is at a range usually below 100 nm. In simple terms, a nanometer is one billionth of a meter and the properties of materials at this atomic or subatomic level differ significantly from properties of the same materials at larger sizes. Although, the initial properties of nanomaterials studied were for its physical, mechanical, electrical, magnetic, chemical and biological applications, recently, attention has been geared towards its pharmaceutical application, especially in the area of drug delivery [1].

According to the definition from NNI (National Nanotechnology Initiative), nanoparticles are structures of sizes ranging from 1 to 100 nm in at least one dimension. However, the prefix "nano" is commonly used for particles that are up to several hundred nanometers in size. Nanocarriers with optimized physicochemical and biological properties are taken up by cells more easily than larger molecules, so they can be successfully used as delivery tools for currently available bioactive compounds [2].

Cell-specific targeting can be achieved by attaching drugs to individually designed carriers. Recent developments in nanotechnology have shown that nanoparticles (structures smaller than 100 nm in at least one dimension) have a great potential as drug carriers. Due to their small sizes, the nanostructures exhibit unique physicochemical and biological properties (e.g., an enhanced reactive area as well as an ability to cross cell and tissue barriers) that make them a favorable material for biomedical applications [3].

It is difficult to use large size materials in drug delivery because of their poor bioavailability, in vivo solubility, stability, intestinal absorption, sustained and targeted delivery, plasma fluctuations, therapeutic effectiveness etc. To overcome these challanges nanodrug delivery have been designed through the development and fabrication of nanostructures. Nanoparticles have the ability to penetrate tissues, and are easily taken up by cells, which allows efficient delivery of drugs to target site of action. Uptake of nanostructures has been reported to be 15–250 times greater than that of microparticles in the 1–10 um range [1]. Nanoparticles can mimic or alter biological processes (e.g., infection, tissue engineering, *de novo* synthesis, etc.). These devices include, but not

limited to, functionalized carbon nanotubes, nanofibers, self-assembling polymeric nanoconstructs, nanomembranes, and nano-sized silicon chips for drug, protein, nucleic acid, or peptide delivery and release, and biosensors and laboratory diagnostics [4].

Various polymers have been used in the design of drug delivery system as they can effectively deliver the drug to a target site and thus increase the therapeutic benefit, while minimizing side effects. The controlled release (CR) of pharmacologically active agents to the specific site of action at the therapeutically optimal rate and dose regimen has been a major goal in designing such devices. The drug is dissolved, entrapped, encapsulated or attached to a NP matrix and depending upon the method of preparation, nanoparticles, nanospheres or nanocapsules can be obtained. Nanocapsules are vesicular systems in which the drug is confined to a cavity surrounded by a unique polymer membrane, while nanospheres are matrix systems in which the drug is physically and uniformly dispersed.

Biodegradable polymeric nanoparticles have attracted considerable attention as potential drug delivery devices in view of their applications in the controlled release of drugs, their ability to target particular organs/tissues, as carriers of DNA in gene therapy, and in their ability to deliver proteins, peptides and genes through a peroral route of administration [5].

Types of Nanoformulations

1) **Fullerenes:** A fullerene is any molecule composed entirely of carbon, in the form of a hollow sphere, ellipsoid, or tube. Spherical fullerenes are also called buckyballs, and cylindrical ones are called carbon nanotubes or buckytubes. Fullerenes are similar in structure to the graphite, which is composed of stacked grapheme sheets of linked hexagonal rings, additionally they may also contain pentagonal (or sometimes heptagonal) rings to give potentially porous molecules [6]. Bucky ball clusters or bucky balls composed of less than 300 carbon atoms are commonly known as endohedral fullerenes and include the most common fullerene, buck minster fullerene, C_{60}. Megatubes are larger in diameter than nanotubes and prepared with walls of different thickness which is potentially used for the transport of a variety of molecules of different sizes [7]. Nano ‘‘onions’’ are spherical particles based on multiple carbon layers surrounding a buckyball core which are proposed for lubricants [8].

2) **Solid lipid nanoparticles (SLNs):** SLNs (solid lipid nanoparticles), NLC (nanostructured lipid carriers) and LDC (lipid drug conjugates) are types of carrier systems based on solid lipid matrix, i.e., lipids solid at the body temperature [9]. SLNs are particles made of solid lipids, e.g., highly purified triglycerides, complex glyceride mixtures or waxes stabilized by various surfactants [10]. The main characteristics of SLN include a good physical stability, protection of incorporated drugs from degradation, controlled drug release, and good tolerability. They have been exploited for the dermal, peroral, parenteral, ocular, pulmonary, and rectal delivery.
3) **Polymeric nanoparticles:** Polymeric nanoparticles (PNPs) are structures with a diameter ranging from 10 to 100 nm. The PNPs are obtained from synthetic polymers, such as poly e-caprolactone, polyacrylamide and polyacrylate, or natural polymers, e.g., albumin, DNA, chitosan, gelatin. Based on in vivo behavior, PNPs may be classified as biodegradable, i.e., poly (L-lactide) (PLA), polyglycolide (PGA), and non-biodegradable, e.g., polyurethane. Drugs can be immobilized on PNPs surface after a polymerization reaction [11] or can be encapsulated on PNP structure during a polymerization step [12]. Nanocarriers composed of biodegradable polymers undergo hydrolysis in the body, producing biodegradable metabolite monomers, such as lactic acid and glycolic acid. Drug-biodegradable polymeric nanocarrier conjugates used for drug delivery are stable in blood, non-toxic, and non-thrombogenic. They are also non-immunogenic as well as non-proinflammatory, and they neither activate neutrophils nor affect reticuloendothelial system [13].
4) **Liposomes:** Liposomes are vesicular structures with an aqueous core surrounded by a hydrophobic lipid bilayer, created by the extrusion of phospholipids. Phospholipids are GRAS (generally recognized as safe) ingredients, therefore minimizing the potential for adverse effects. Solutes, such as drugs, in the core cannot pass through the hydrophobic bilayer however hydrophobic molecules can be absorbed into the bilayer, enabling the liposome to carry both hydrophilic and hydrophobic molecules. The lipid bilayer of liposomes can fuse with other bilayers such as the cell membrane, which promotes release of its contents, making them

useful for drug delivery and cosmetic delivery applications. Liposomes that have vesicles in the range of nanometers are also called nanoliposomes [14]. Liposomes can vary in size, from 15 nm up to several μm and can have either a single layer (unilamellar) or multiple phospholipid bilayer membranes (multilamellar) structure. Unilamellar vesicles (ULVs) can be further classified into small unilamellar vesicles (SUVs) and large unilamellar vesicles (LUVs) depending on their size range. Liposome surface can be easily functionalized with 'stealth' material to enhance their in vivo stability or targeting ligands to enable preferential delivery of liposomes. These versatile properties of liposomes made them to be useful as potent carrier for various drugs like antibacterials, antivirals, insulin, antineoplastics and plasmid DNA.

5) **Nanoshells:** Nanoshells are spherical cores of a particular compound (concentric particles) surrounded by a shell or outer coating of thin layer of another material, which is few nanometers (1–20 nm) thick. Nanoshell materials can be synthesized from semiconductors (dielectric materials such as silica and polystyrene), metals and insulators. Usually dielectric materials such as silica and polystyrene are commonly used as core because they are highly stable [15]. Nanoshells possess highly favorable optical and chemical properties for biomedical imaging and therapeutic applications. Nanoshells offer other advantages over conventional organic dyes including improved optical properties and reduced susceptibility to chemical/thermal denaturation [16].
6) **Quantum dots (QD):** The quantum dots are semiconductor nanocrystals and coreshell nanocrystals containing interface between different semiconductor materials. The size of quantum dots can be continuously tuned from 2 to 10 nm, which, after polymer encapsulation, generally increases to 5–20 nm in diameter. Particles smaller than 5 nm are quickly cleared by renal filtration [17]. QD core can serve as the structural scaffold, and the imaging contrast agent and small molecule hydrophobic drugs can be embedded between the inorganic core and the amphiphilic polymer coating layer. Hydrophilic therapeutic agents, including small interfering RNA (siRNA), antisense oligodeoxynucleotide (ODN)) and targeting biomolecules such as antibodies, peptides and aptamers can be immobilized onto

the hydrophilic side of the amphiphilic polymer via either covalent or non-covalent bonds. This fully integrated nanostructure may behave like magic bullets that will not only identify, but bind to diseased cells and treat them. It will also emit detectable signals for real-time monitoring of its trajectory [18].

7) **Carbon nanomaterials:** Carbon nanocarriers used in DDS are differentiated into nanotubes (CNTs) and nanohorns (CNH). CNTs are characterized by unique architecture formed by rolling of single (SWNCTs – single walled carbon nanotubes) or multi (MWCNTs – multi walled carbon nanotubes) layers of graphite with an enormous surface area and an excellent electronic and thermal conductivity [19]. There are three ways of drug immobilization in carbon nanocarriers, which are: encapsulation of a drug in the carbon nanotube [20, 21], chemical adsorption on the surface or in the spaces between the nanotubes (by electrostatic, hydrophobic, π-π interactions and hydrogen bonds) [22, 23], and attachment of active agents to functionalized carbon nanotubes (f-CNTs). Encapsulation has the advantage over the two remaining methods as the drug is protected from degradation during its transport to the cells and is released only in specific conditions [24]. Nanohorns – a type of the only single-wall nanotubes – exhibit similar properties to nanotubes. Their formation process does not require a metal catalyst, thus, they can be easily prepared with very low cost and are of high purity. The immobilization of drugs may rely on adsorption on nanohorn walls or nanoprecipitation of drugs with nanohorns [25].
8) **Superparamagnetic nanoparticles:** Superparamagnetic molecules are those that are attracted to a magnetic field but do not retain residual magnetism after the field is removed. Nanoparticles of iron oxide with diameters in the 5–100 nm range have been used for selective magnetic bioseparations. Typical techniques involve coating the particles with antibodies to cell-specific antigens, for separation from the surrounding matrix. Superparamagnetic nanoparticles belong to the class of inorganic based particles having an iron oxide core coated by either inorganic materials (silica, gold) and organic (phospholipids, fatty acids, polysaccharides, peptides or other surfactants and polymers) [26, 27, 28]. In contrast to other nanoparticles, supramagnetic nanoparticles based on their inducible magnetization,

their magnetic properties allow them to be directed to a defined location or heated in the presence of an externally applied AC magnetic field. These characteristics make them attractive for many applications, ranging from various separation techniques and contrast enhancing agents for MRI to drug delivery systems, magnetic hyperthermia (local heat source in the case of tumor therapy), and magnetically assisted transfection of cells [29, 30, 31]. The main advantages of superparamagnetic nanoparticles are that they can be visualized in magnetic resonance imaging (MRI) due to their paramagnetic properties; they can be guided to a location by the use of magnetic field and heated by magnetic field to trigger the drug release [32].

9) **Dendrimers:** Dendrimers are unimolecular, monodisperse, micellar nanostructures, around 20 nm in size, with a well-defined, regularly branched symmetrical structure and a high density of functional end groups at their periphery. The structure of dendrimers consists of three distinct architectural regions as a focal moiety or a core, layers of branched repeat units emerging from the core, and functional end groups on the outer layer of repeat units. They are known to be robust, covalently fixed, three dimensional structures possessing both a solvent-filled interior core (nanoscale container) as well as a homogenous, mathematically defined, exterior surface functionality [33, 34]. There are a few ways of connecting biologically active compounds to dendrimers. The drug may be encapsulated in the internal structure of dendrimers [35] or it can be chemically attached or physically adsorbed on dendrimers surface [36]. The choice of the immobilization method depends on the drug properties. Encapsulation is used when drugs are labile, toxic, or poorly soluble. In turn, chemical attachment provides the possibility to control quantity of drugs on dendrimers surface by controlling the number of covalent bonds [37]. Dendrimeric vectors are most commonly used as parenteral injections, either directly into the tumor tissue or intravenously for systemic delivery [38]. Dendrimers used in drug delivery studies typically incorporate one or more of the following polymers: polyamidoamine (PAMAM), melamine, poly L-glutamicacid (PG), polyethyleneimine (PEI), polypropyleneimine (PPI), polyethylene glycol (PEG) and chitin. Dendrimers may be used in two major modalities for targeting

vectors for diagnostic imaging, drug delivery, gene transfection also detection and therapeutic treatment of cancer and other diseases.

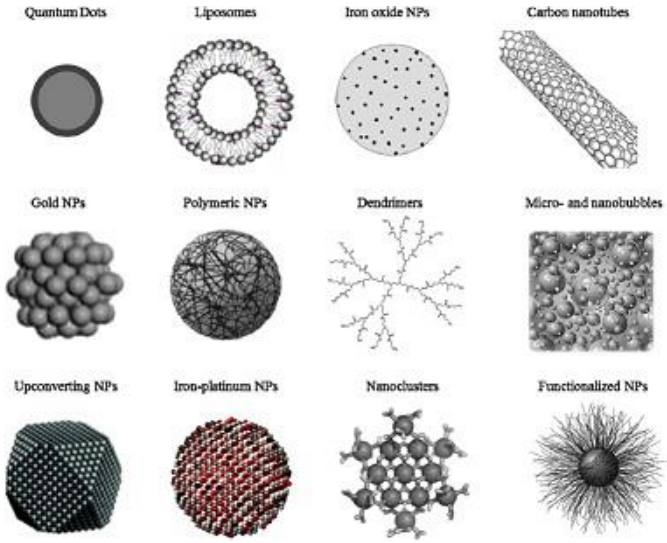

Fig 1.1 Different nanocarriers used in medicine (source: www.bargozideha.com)

Table 1.1 Various natural and synthetic polymers used for the preparation of NPs

Natural	**Synthetic**
Gelatin	Polylactides (PLA)
Albumin	Polyglycolides (PGA)
Chitosan	Poly(lactide-co-glycolides) or PLGA
Sodium alginate	Polyanhydrides
Lecithin	Polycyanocreylates
Legumin	Polycaprolactone
Vicillin	Poly(ethylene glycol)

1.2 Preparation of Nanoparticles:

The polymeric nanoparticles (PNPs) are prepared from biocompatible and biodegradable polymers in size between 10-1000 nm where the drug is dissolved, entrapped, encapsulated or attached to a nanoparticle matrix. In order to achieve the properties of interest, the mode of preparation plays a vital role. Thus, it is highly advantageous to have preparation techniques at hand to obtain PNPs with the desired properties for a particular application. The selection of the appropriate method for the preparation of nanoparticles depends on the physicochemical characteristics of the polymer and the drug to be loaded. The following methods are used for preparation of nanoparticles:

1.2.1 Methods for preparation of nanoparticles from dispersion of preformed polymer

a) Solvent evaporation

b) Nanoprecipitation

c) Emulsification/solvent diffusion

d) Salting out

e) Dialysis

f) Supercritical fluid technology (SCF)

a) Solvent evaporation: In this method, polymer solutions are prepared in volatile solvents and emulsions are formulated. The emulsion is converted into a nanoparticle suspension on evaporation of the solvent for the polymer, which is allowed to diffuse through the continuous phase of the emulsion. In the conventional methods, two main strategies are being used for the formation of emulsions, the preparation of single-emulsions, e.g., oil-in-water (o/w) or double-emulsions, e.g., (water-in-oil)-in-water, (w/o)/w. These methods utilize high-speed homogenization or ultrasonication, followed by evaporation of the solvent, either by continuous magnetic stirring at room temperature or under reduced pressure. Afterwards, the solidified nanoparticles can be collected by ultracentrifugation and washed with distilled water to remove additives such as surfactants. Finally, the product is lyophilized [39].

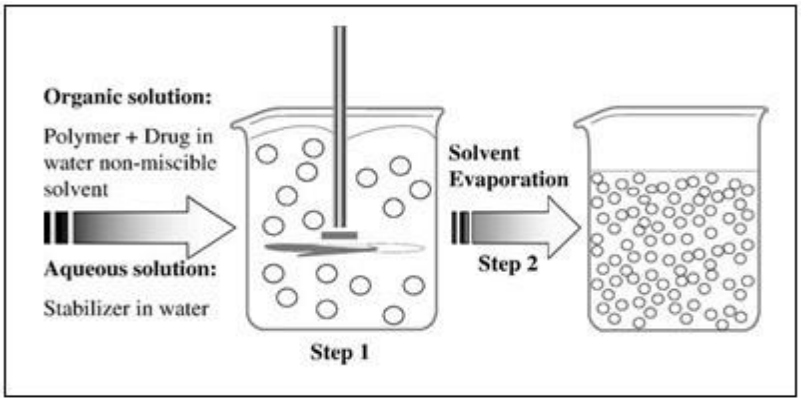

Fig 1.2 Schematic representation of the solvent-evaporation technique [Ref: Catarina *et al 2006*].

b) Nanoprecipitation: Nanoprecipitation is also called solvent displacement method. It involves the precipitation of a preformed polymer from an organic solution and the diffusion of the organic solvent in the aqueous medium in the presence or absence of a surfactant [40]. The polymer generally PLA, is dissolved in a water-miscible solvent of intermediate polarity, leading to the precipitation of nanospheres. This phase is injected into a stirred aqueous solution containing a stabilizer as a surfactant. Polymer deposition on the interface between water and the organic solvent, caused by fast diffusion of the solvent, leads to the instantaneous formation of a colloidal suspension [41]. To facilitate the formation of colloidal polymer particles during the first step of

the procedure, phase separation is performed with a totally miscible solvent that is also a non-solvent of the polymer [42]. The solvent displacement technique allows the preparation of nanocapsules when a small volume of nontoxic oil is incorporated in the organic phase. Considering the oil-based central cavities of the nanocapsules, high loading efficiencies are generally reported for lipophilic drugs when nanocapsules are prepared. The usefulness of this simple technique is limited to water-miscible solvents, in which the diffusion rate is enough to produce spontaneous emulsification [41].

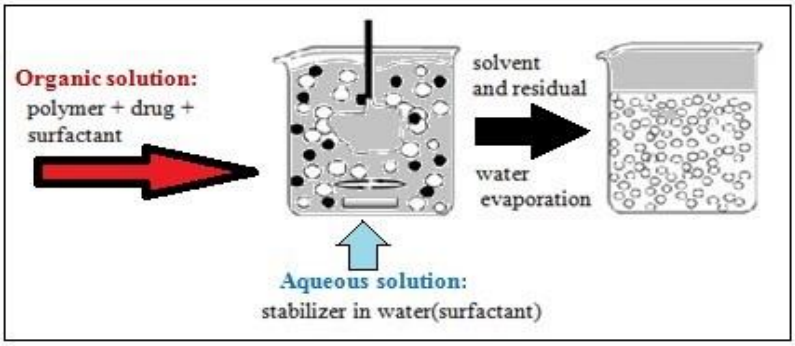

Fig 1.3 Schematic representation of the nanoprecipitation technique [Ref: Nagavarma *et al 2012*].

c) Emulsification/solvent diffusion (ESD): This is a modified version of solvent evaporation method. The encapsulating polymer is dissolved in a partially water soluble solvent such as propylene carbonate and saturated with water to ensure the initial thermodynamic equilibrium of both liquids. In fact, to produce the precipitation of the polymer and the consequent formation of nanoparticles, it is necessary to promote the diffusion of the solvent of the dispersed phase by dilution with an excess of water when the organic solvent is partly miscible with water or with another organic solvent in the opposite case. Subsequently, the polymer-water saturated solvent phase is emulsified in an aqueous solution containing stabilizer, leading to solvent diffusion to the external phase and the formation of nanospheres or nanocapsules, according to the oil-to-polymer ratio. Finally, the solvent is eliminated by evaporation or filtration, according to its boiling point. This technique presents several advantages, such as high encapsulation efficiencies (generally >70%), no need for homogenization, high batch-to-batch reproducibility, ease of scale-up, simplicity, and narrow size distribution. Disadvantages are the high volumes of water to be eliminated from the suspension and the leakage of water-soluble drug into the saturated-aqueous external phase during emulsification, reducing encapsulation efficiency [43].

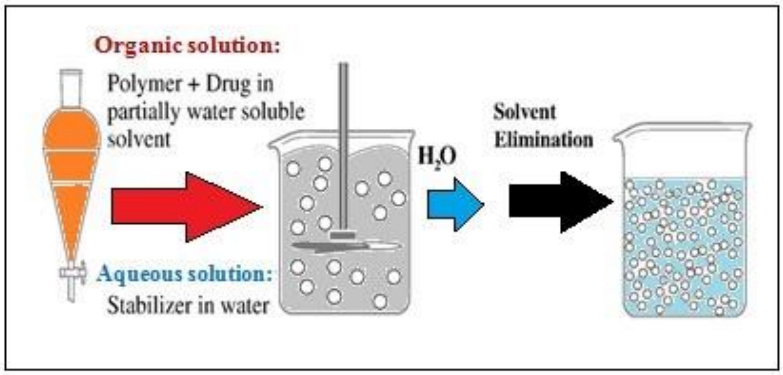

Fig 1.4 Schematic representation of the emulsification/solvent diffusion technique [Ref: Nagavarma *et al 2012*].

d) Salting out: Salting out is based on the separation of a water miscible solvent from aqueous solution via a salting out effect. Polymer and drug are initially dissolved in a solvent such as acetone, which is subsequently emulsified into an aqueous gel containing the salting-out agent (electrolytes, such as magnesium chloride, calcium chloride, and magnesium acetate, or non-electrolytes such as sucrose) and a colloidal stabilizer such as polyvinylpyrrolidone or hydroxyethylcellulose. This oil/water emulsion is diluted with a sufficient volume of water or aqueous solution to enhance the diffusion of acetone into the aqueous phase, thus inducing the formation of nanospheres [39]. The selection of the salting out agent is important, because it can play an important role in the encapsulation efficiency of the drug. Both the solvent and the salting out agent are then eliminated by cross-flow filtration. This technique used in the preparation of PLA, poly (methacrylic) acid, nanospheres leads to high efficiency and is easily scaled up. The main advantage of salting out is that it minimizes stress to protein encapsulants [44]. Salting out does not require an increase of temperature and therefore, may be useful when heat sensitive substances have to be processed [45]. The greatest disadvantages are exclusive application to lipophilic drugs and the extensive nanoparticle washing steps [46].

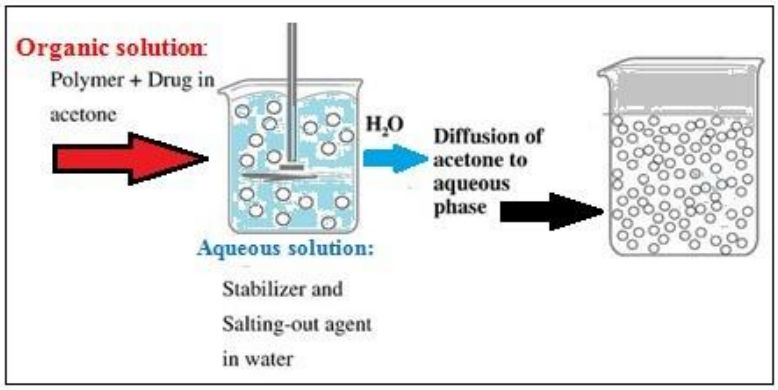

Fig 1.5 Schematic representation of the salting out technique [Ref: Nagavarma *et al 2012*].

e) Dialysis: In this method, polymer is dissolved in an organic solvent and placed inside a dialysis tube with proper molecular weight cut off. Dialysis is performed against a non-solvent miscible with the former miscible. The displacement of the solvent inside the membrane is followed by the progressive aggregation of polymer due to a loss of solubility and the formation of homogeneous suspensions of nanoparticles.

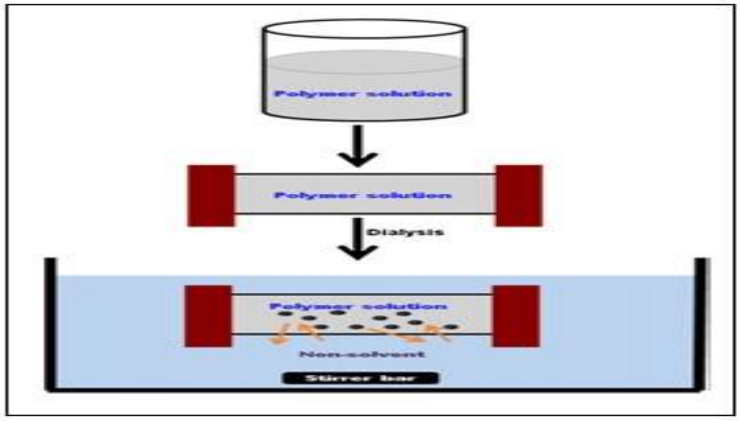

Fig 1.6 Schematic representation of dialysis method [Ref: Rao *et al 2011*].

f) Supercritical fluid technology: Supercritical fluids are environmental friendly solvents, and are capable to produce PNPs with high purity without using any organic solvent. The production of nanoparticles using supercritical fluids involves two principles:

i) **Rapid expansion of supercritical solution (RESS)**: In this method, the solute is dissolved in a supercritical fluid to form a solution, followed by the rapid expansion of the solution across an orifice or a capillary nozzle into ambient air. The high degree of super saturation, accompanied by the rapid pressure reduction in the expansion, results in homogenous nucleation and thereby, the formation of well-dispersed particles. The RESS experimental apparatus consists of three major units: a high-pressure stainless steel mixing cell, a syringe pump, and a pre-expansion unit. A solution of polymer in CO_2 is prepared at ambient temperature. Before the solution leaves the nozzle, using syringe pump, it is pumped to the pre-expansion unit and is heated isobarically to the pre-expansion temperature. The supercritical solution is now allowed to expand through the nozzle, at ambient pressure. The concentration and degree of saturation of

the polymer have a considerable effect on the particle size and morphology of the particles for RESS [47].

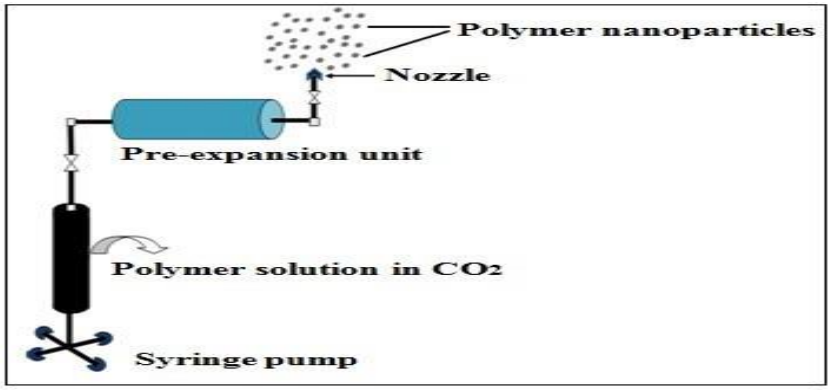

Fig 1.7 Experimental set-up for preparation of PNPs by rapid expansion of supercritical fluid solution [Ref: Rao *et al 2011*].

ii) Rapid expansion of supercritical solution into liquid solvent (RESOLV): This is the modified form of RESS, which involves expansion of the supercritical solution into a liquid solvent instead of ambient air. In RESOLV the liquid solvent apparently suppresses the particle growth in the expansion jet, thus making it possible to obtain primarily nanosized particles.

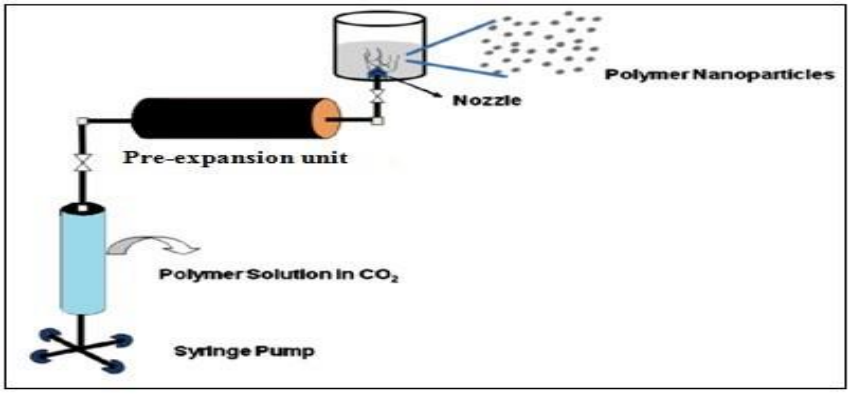

Fig 1.8 Experimental set-up for the rapid expansion of supercritical fluid solution into liquid solvent process [Ref: Rao *et al 2011*].

1.2.2 Methods for preparation of nanoparticles from polymerization of monomers

a) Emulsion

b) Mini emulsion

c) Micro emulsion

d) Interfacial polymerization

a) Emulsion polymerization: This is the readily scalable and rapid method for nanoparticle preparation. The method is classified into two categories, based on the use of an organic or aqueous continuous phase. The continuous organic phase methodology involves the dispersion of monomer into an emulsion or inverse microemulsion, or into a material in which the monomer is not soluble. This procedure has many drawbacks, because it requires toxic organic solvents, surfactants, monomers and initiator, which are subsequently eliminated from the formed particles. In the aqueous continuous phase the monomer is dissolved in a continuous phase that is usually an aqueous solution, and the surfactants or emulsifiers are not needed. Initiation occurs when a monomer molecule dissolved in the continuous phase collides with an initiator molecule that might be an ion or a free radical. Alternatively, the monomer molecule can be transformed into an initiating radical by high-energy radiation, including gamma-radiation, or ultraviolet or strong visible light. Chain growth starts when initiated monomer ions or monomer radicals collide with other monomer molecules according to an anionic polymerization mechanism. Phase separation and formation of solid particles can take place before or after termination of the polymerization reaction [39, 48].

b) Mini-emulsion polymerization: The formulation used in mini- emulsion polymerization consists of water, monomer mixture, co-stabilizer, surfactant, and initiator. The main difference between emulsion polymerization and mini-emulsion polymerization is the utilization of a low molecular mass compound as the co-stabilizer and also the use of a high-shear device (ultrasound, etc.). Mini-emulsions are critically stabilized, require a high-shear to reach a steady state and have an interfacial tension much greater than zero [49].

c) Micro-emulsion polymerization: In micro-emulsion polymerization, an initiator, typically water-soluble, is added to the aqueous phase of a thermodynamically stable micro-emulsion containing swollen micelles. The polymerization starts from this thermodynamically stable, spontaneously formed state and relies on high quantities of surfactant systems, which possess an interfacial tension at the oil/water interface close to zero [50].

d) Interfacial polymerization: It involves step polymerization of two reactive monomers or agents, which are dissolved respectively in two phases (i.e., continuous- and dispersed-phase), and

the reaction takes place at the interface of the two liquids. Oil-containing nanocapsules were obtained by the polymerization of monomers at the oil/water interface of a very fine oil-in-water micro- emulsion, while water-containing nanocapsules can be obtained by the interfacial polymerization of monomers in water-in-oil micro-emulsions [51].

1.2.3 Ionic gelation or coacervation of hydrophilic polymers: Polymeric nanoparticles are prepared by using biodegradable hydrophilic polymers such as chitosan, gelatin and sodium alginate. This method involves a mixture of two aqueous phases, of which one is the polymer chitosan, a di-block co-polymer ethylene oxide or propylene oxide (PEO-PPO) and the other is a poly anion sodium tripolyphosphate. In this method, positively charged amino group of chitosan interacts with negative charged tripolyphosphate to form coacervates with a size in the range of nanometer. Coacervates are formed as a result of electrostatic interaction between two aqueous phases, whereas, ionic gelation involves the material undergoing transition from liquid to gel due to ionic interaction conditions at room temperature [52].

1.3 Important characteristics for drug delivery using nanoparticles: Generally, particle size, morphology, and surface charge are some important parameters in the characterization of nanoparticles using some advanced microscopic techniques such as scanning electron microscopy (SEM), transmission electron microscopy (TEM) and atomic force microscopy (AFM). The average particle diameter, their size distribution and charge affect the physical stability and the *in vivo* distribution of the nanoparticles. The surface charge of the nanoparticles plays an important role in the physical stability and redispersibility of the polymer dispersion as well as their *in vivo* performance. Some important characterization parameters of nanoparticles are discussed below:

a) Particle size: Particle size and size distribution are the most important characteristics of nanoparticles, as they have major impact on *in vivo* distribution, biological fate, toxicity and targeting ability of these delivery systems. In addition they can influence drug loading, drug release and stability of nanoparticles. Smaller particles have a larger surface area-to-volume ratio; therefore most of the drug loaded on to them would be at or near the particle surface, leading to faster drug release. On the other hand, larger particles have large cores, which allow more drug to be encapsulated per particle and give slower release. Thus particle size of the nanoparticle must be controlled to get the desired drug release rate. As a drawback, smaller particles tend to aggregate during storage and transportation of nanoparticle dispersion. Hence, there is a compromise

between a small size and maximum stability of nanoparticles [53]. Polymer degradation can also be affected by the particle size. It has been reported that the degradation rate of poly (lactic-co-glycolic acid) was found to increase with increasing particle size *in vitro* [54].

b) Surface charge: The surface charge of the nanoparticles plays an important role in the determination of interaction of the nanoparticles with the biological environment as well as their electrostatic interaction with the bioactive compounds. Zeta potential is an indirect measure of surface charge and it determines the colloidal stability of nanoparticles. High zeta potential values, either positive or negative, should be achieved in order to ensure stability and avoid aggregation of the particles [55].

c) Surface hydrophobicity: The extent of surface hydrophobicity can be predicted from the values of zeta potential. Surface hydrophobicity can be determined by several techniques such as hydrophobic interaction chromatography, biphasic partitioning, adsorption of probes, contact angle measurements etc. X-Ray photon correlation spectroscopy permits the identification of specific chemical groups on the surface of nanoparticles [56].

d) Drug loading: A successful nanoparticulate system should have a high drug-loading capacity thereby reduce the quantity of matrix materials for administration. Drug loading can be done by two methods: one, by incorporating the drug at the time of NP production or secondly, by adsorbing the drug after the formulation of NPs by incubating them in the drug solution. A larger amount of drug can be entrapped by the incorporation method than the adsorption. Drug loading and entrapment efficiency very much depend on the solid-state drug solubility in matrix material or polymer (solid dissolution or dispersion), which is related to the polymer composition, the molecular weight, the drug polymer interaction and the presence of end functional groups (ester or carboxyl) [57].

e) Drug release: Drug release and polymer biodegradation, both are important in the development of nanoparticulate delivery system. In general, the drug release rate depends on: (a) drug solubility; (b) desorption of surface-bound or adsorbed drug; (c) drug diffusion through the nanoparticle matrix; (d) nanoparticle matrix erosion or degradation; and (e) the combination of erosion and diffusion processes. In the case of nanospheres, where the drug is uniformly distributed, drug release occurs by diffusion or erosion of the matrix. If the diffusion of the drug is faster than matrix erosion, then the mechanism of release is largely controlled by a diffusion process. The rapid,

initial release, or 'burst', is mainly attributed to weakly bound or adsorbed drug to the relatively large surface of nanoparticles [58]. It is evident that the method of incorporation has an effect on the release profile. If the drug is loaded by the incorporation method, then the system has a relatively small burst effect and sustained release characteristics [59]. If the nanoparticle is coated by polymer, the release is then controlled by diffusion of the drug from the polymeric membrane. Various methods can be used to study the release of drug from the nanoparticle:

(i) Side-by-side diffusion cells with artificial or biological membranes.

(ii) Dialysis bag diffusion.

(iii) Reverse dialysis bag diffusion.

(iv) Agitation followed by ultracentrifugation/centrifugation.

(v) Ultra-filtration.

Commonly release study is carried out by controlled agitation and centrifugation. As the method is time consuming and technical difficulties encountered in the separation of nanoparticles from release media, the dialysis technique is generally preferred.

1.4 Therapeutic Applications of Nanoparticles

a) Oral delivery: Oral drug delivery is the oldest and commonest mode of drug administration as it is safer, more convenient, does not need assistance, non-invasive, often painless, the medicament needs not to be sterile and so is cheaper. However, the oral route is not suitable for drugs that are poorly permeable or easily degradable in the gastrointestinal tracts (GIT). For instance, delivery of proteins and peptides via the oral route will be greatly affected by barriers such as epithelial cell lining, the mucus layer, proteolytic enzymes etc. Drug loaded in nanoparticles will be protected from enzymatic degradation along the GIT providing the potential benefit of enhanced absorption. It has been reported that particulate absorption takes place mainly at the intestinal lymphatic tissues (the Peyer's patches). The epithelial cell layer overlying the Peyer's patches contains microfold cell (M cells). The differences between absorptive enterocytes and M cells are expressed in that M cells have (a) underdeveloped microvillous and glycocalyx structures, (b) apical microfolds, (c) increased intracellular vacuolization and (d) absence of mucus. The follicle-associated epithelia

(FAE) are made up of the M cells and absorptive enterocytes. The FAE and M cells are predominantly responsible for particle uptake along the GIT. In this regard, nanotechnology is reportedly gaining attention in the development of proteins, peptides and DNA delivery systems [60].

b) Pulmonary administration: The small size of nanoparticles makes them highly suitable for pulmonary delivery because they can easily be air borne and delivered to the alveolus. If a drug is prepared as microspheres in the size range of 7-25 µm, the microspheres can be concentrated in lung through i.v. administration [61]. This technique can be useful in some pulmonary infections such as mycoplasmal pneumonia and minimize the adverse side effects. The final nanoparticulate formulation may be administered either as a nebulizer or dry powder inhalers. By delivering the drug locally to the lung in a sustained and controlled manner, nanoparticulate formulations are useful in many clinical conditions such as asthma, chronic pulmonary infections, lung cancer and cystic fibrosis.

c) Brain delivery: The blood--brain barrier (BBB) represents an insurmountable obstacle for a large number of drugs, including antibiotics, antineoplastic agents, and a variety of central nervous system (CNS)-active drugs, especially neuropeptides. One of the possibilities to overcome this barrier is a drug delivery to the brain using nanoparticles. Kreuter et al (1982) were able to deliver several drugs successfully through the blood–brain barrier using polysorbate 80-coated poly (butylcyanoacrylate) nanoparticles [48]. Nanoparticle-mediated drug transport to the brain depends on the overcoating of the particles with polysorbates, especially polysorbate 80. Overcoating with these materials seems to lead to the adsorption of apolipoprotein E (APOE) from blood plasma onto the nanoparticle surface. The particles then seem to mimic low density lipoprotein (LDL) particles and could interact with the LDL receptor leading to their uptake by the endothelial cells. After this the drug may release in these cells and diffuses into the brain interior or the particles may be transcytosed. Other processes such as tight junction modulation or P-glycoprotein (Pgp) inhibition also may occur [62].

d) Cancer therapy: Photodynamic cancer therapy is based on the destruction of the cancer cells by laser generated atomic oxygen, which is cytotoxic. A greater quantity of a special dye that is used to generate the atomic oxygen is taken in by the cancer cells when compared with a healthy tissue. Hence, only the cancer cells are destroyed then exposed to a laser radiation. Unfortunately,

the remaining dye molecules migrate to the skin and the eyes and make the patient very sensitive to the daylight exposure. This effect can last for up to six weeks. To avoid this side effect, the hydrophobic version of the dye molecule was enclosed inside a porous nanoparticle. The dye stayed trapped inside the Ormosil nanoparticle and did not spread to the other parts of the body. At the same time, its oxygen generating ability has not been affected and the pore size of about 1 nm freely allowed for the oxygen to diffuse out [63].

e) Multicolour optical coding for biological assays: Single quantum dots of compound semiconductors were successfully used as a replacement of organic dyes in various bio-tagging applications. This idea has been taken one step further by Han et.al. (2001) by combining differently sized and hence having different fluorescent colours quantum dots, and combining them in polymeric microbeads [64]. A precise control of quantum dot ratios has been achieved. The selection of nanoparticles used in those experiments had 6 different colours as well as 10 intensities. It is enough to encode over 1 million combinations. The uniformity and reproducibility of beads was high letting for the bead identification accuracies of 99.99%.

f) Manipulation of cells and biomolecules: Functionalised magnetic nanoparticles have been found in many applications including cell separation and probing. Most of the magnetic particles studied so far are spherical, which somewhat limits the possibilities to make these nanoparticles multifunctional. Alternative cylindrically shaped nanoparticles can be created by employing metal electrodeposition into nanoporous alumina template [65]. By sequentially depositing various thicknesses of different metals, the structure and the magnetic properties of individual cylinders can be tuned widely. As surface chemistry for functionalisation of metal surfaces is well developed, different ligands can be selectively attached to different segments. For example, porphyrins with thiol or carboxyl linkers were simultaneously attached to the gold or nickel segments respectively. It has been shown that a self-assembly of magnetic nanowires in suspension can be controlled by weak external magnetic fields. This would potentially allow controlling cell assembly in different shapes and forms. Moreover, an external magnetic field can be combined with a lithographically defined magnetic pattern ("magnetic trapping").

g) Protein detection: Proteins are the important part of the cell's language, machinery and structure, and understanding their functionalities is extremely important for further progress in human well-being. Gold nanoparticles are widely used in immunohistochemistry to identify

protein-protein interaction. However, the multiple simultaneous detection capabilities of this technique are fairly limited. Surface-enhanced Raman scattering spectroscopy is a well-established technique for detection and identification of single dye molecules. By combining both methods in a single nanoparticle probe one can drastically improve the multiplexing capabilities of protein probes [66].

REFERENCES

1. Martins, O.E., Ifeoma, C.O., Ekaete, I.A., Sabinus, I.O., 2012. Nanotechnology in Drug Delivery. Intech, http://dx.doi.org/10.5772/51384, 69.
2. Suri, S.S., Fenniri, H., Singh, B., 2007. Nanotechnology-based drug delivery systems. J Occup Med Toxicol, 2, 16.
3. Agnieszka, Z.W., Katarzyna, N., Karolina, H.M., Halina, C., 2012. Nanoparticles as drug delivery systems. Pharmacological Reports, 64, 1020-1037.
4. Singh, R., James, W.L.Jr., 2009. Nanoparticle-based targeted drug delivery. Exp Mol Pathol, 86, 215-223.
5. Langer, R., 2000. Biomaterials in drug delivery and tissue engineering: One laboratory's experience. Acc. Chem. Res., 33, 94–101.
6. Mudshinge, S.R., Deore, A.B., Patil, S., Bhalgat, C.M., 2011. Nanoparticles: Emerging carriers for drug delivery. SPJ, 19, 129–141.
7. Mitchell, D.R., Brown, Jr. R.M., Spires, T.L., Romanovicz, D.K., Lagow, R.J., 2001. The synthesis of megatubes: new dimensions in carbon materials. Inorg. Chem. 40, 2751–2755.
8. Sano, N., Wang, H., Chhowalla, M., Alexandrou, I., Amaratunga, G.A.J., 2001. Synthesis of carbon 'onions' in water. Nature 414, 506–507.
9. Wissing, S.A., Kayser, O., Muller, R.H., 2004. Solid lipid nanoparticles for parenteral drug delivery. Adv Drug Deliv Rev, 56, 1257–1272.
10. Mukherjee, S., Ray, S., Thakur, R.S., 2009. Solid Lipid Nanoparticles: A Modern Formulation Approach in Drug Delivery System. Indian J Pharm Sci., 71, 349-358.
11. Luo, X., Matranga, C., Tan, S., Alba, N., Cui, X.T., 2011. Carbon nanotube nanoreservior for controlled release of anti-inflammatory dexamethasone. Biomaterials, 32, 6316–6323.
12. Mora-Huertas, C.E., Fessi, H., Elaissari, A., 2010. Polymer-based nanocapsules for drug delivery. Int J Pharm, 385, 113–142.
13. des Rieux, A., Fievez, V., Garinot, M., Schneider, Y.J., Preat, V., 2006. Nanoparticles as potential oral delivery systems of proteins and vaccines: a mechanistic approach. J Control Release, 116, 1–27.
14. Zhang, L., Granick, S., 2006. How to stabilize phospholipid liposomes (using nanoparticles). Nano Lett. 6, 694–698.
15. Kalele, S.A., Gosavi, S.W., Urban, J., Kulkarni, S.K., 2006. Nanoshell particles: synthesis, properties and applications. Curr. Sci. 91, 1038–1052.
16. Loo, C., Lin, A., Hirsch, L., Lee, M., Barton, J., Halas, N., West, J., Drezek, R., 2004. Nanoshell-enabled photonics-based imaging and therapy of cancer. Technol. Cancer Res. Treat. 3, 33–40.
17. Choi, H.S., Liu, W., Misra, P., Tanaka, E., Zimmer, J.P., Ipe, B.I., Bawendi, M.G., Frangion, J.V., 2007. Renal clearance of quantum dots. Nat. Biotechnol. 25, 1165–1170.
18. Qi, L., Gao, X., 2008. Emerging application of quantum dots for drug delivery and therapy. Expert Opin. Drug Deliv. 5, 63–67.
19. Beg, S., Rizwan, M., Sheikh, A.M., Hasnain, M.S., Anwer, K., Kohli, K., 2011. Advancement in carbon nanotubes: basics, biomedical applications and toxicity. J Pharm Pharmacol, 63, 141–163.

20. Arsawang, U., Saengsawang, O., Rungrotmongkol, T., Sornmee, P., Wittayanarakul, K., Remsungnen, T., Hannongbua, S., 2011. How do carbon nanotubes serve as carriers for gemcitabine transport in a drug delivery system? J Mol Graph Model, 29, 591–596.
21. Tripisciano, C., Costa, S., Kalenczuk, R.J., Borowiak-Palen, E., 2010. Cisplatin filled multiwalled carbon nanotubes – a novel molecular hybrid of anticancer drug container. Eur Phys J B, 75, 141–146.
22. Chen, Z., Pierre, D., He, H., Tan, S., Pham-Huy, C., Hong, H., Huang, J., 2011. Adsorption behavior of epirubicin hydrochloride on carboxylated carbon nanotubes. Int J Pharm, 28, 153–161.
23. Zhang, D., Pan, B., Wu, M., Wang, B., Zhang, H., Peng, H., Wu, D., Ning, P., 2011. Adsorption of sulfamethoxazole on functionalized carbon nanotubes as affected by cations and anions. Environ Pollut, 159, 2616–2621.
24. Perry, J.L., Martin, C.R., Stewart, J.D., 2011. Drug-delivery strategies by using template-synthesized nanotubes. Chemistry, 17, 6296–6302.
25. Ajima, K., Murakami, T., Mizoguchi, Y., Tsuchida, K., Ichihashi, T., Iijima, S., Yudasaka, M., 2008. Enhancement of in vivo anticancer effects of cisplatin by incorporation inside singlewall carbon nanohorns. ACS Nano, 2, 2057–2064.
26. Gupta, A.K., Curtis, A.S.G., 2004. Lactoferrin and ceruloplasmin derivatized superparamagnetic iron oxide nanoparticles for targeting cell surface receptors. Biomaterials 25, 3029–3040.
27. Babic, M., Hora´ k, D., Trchova´, M., Jendelova´, P., Glogarova´, K., Lesny´, P., Herynek, V., Ha´ jek, M., Sykova´, E., 2008. Poly (Llysine) - modified iron oxide nanoparticles for stem cell labeling. Bioconjug. Chem. 19, 740–750.
28. Euliss, L.E., Grancharov, S.G., O'Brien, S., Deming, T.J., Stucky, G.D., Murray, C.B., Held, G.A., 2003. Cooperative Assembly of Magnetic Nanoparticles and Block Copolypeptides in Aqueous Media. Nano Lett. 3, 1489–1493.
29. Hora´ k, D., 2005. Magnetic microparticulate carriers with immobilized selective ligands in DNA diagnostics. Polym. 46, 1245–1255.
30. Jordan, A., Scholz, R., Maier-Hauff, K., Johannsen, M., Wust, P., Nadobny, J., Schirra, H., Schmidt, H., Deger, S., Loening, S., Lanksch, W., Felix, R., 2001. Presentation of a new magnetic field therapy system for the treatment of human solid tumors with magnetic fluid hyperthermia. J. Magn. Magn. Mater. 225, 118–126.
31. Neuberger, T., Schopf, B., Hofmann, H., Hofmann, M., von Rechenberg, B., 2005. Superparamagnetic nanoparticles for biomedical applications: possibilities and limitations of a new drug delivery system. J. Magn. Magn. Mater. 293 (1), 483–496.
32. Irving, B., 2007. Nanoparticle drug delivery systems. Inno. Pharm. Biotechnol. 24, 58–62.
33. Grayson, S.M., Frechet, J.M., 2001. Convergent dendrons and dendrimers: from synthesis to applications. Chem. Rev. 101, 3819–3868.
34. Svenson, S., Tomalia, D.A., 2005. Dendrimers in biomedical applications-reflections on the field. Adv. Drug Deliv. Rev. 57, 2106–2129.
35. D'Emanuele, A., Attwood, D., 2005. Dendrimer-drug interactions. Adv Drug Deliv Rev, 57, 2147–2162.

36. Menjoge, A.R., Kannan, R.M., Tomalia, D.A., 2010. Dendrimerbased drug and imaging conjugates: design considerations for nanomedical applications. Drug Discov Today, 15, 171–187.
37. Singh, P., Gupta, U., Asthana, A., Jain, N.K., 2008. Folate and Folate-PEG-PAMAM dendrimers: synthesis, characterization, and targeted anticancer drug delivery potential in tumor bearing mice. Bioconjugate Chem, 19, 2239–2252.
38. Tomalia, D.A., Reyna, L.A., Svenson, S., 2007. Dendrimers as multipurpose nanodevices for oncology drug delivery and diagnostic imaging. Biochem. Soc. Trans. 35, 61–67.
39. Catarina, P.R., Ronald, J.N., Antonio, J.R., Francisco, V., 2006. Nanoencapsulation I. Methods for preparation of drug-loaded polymeric nanoparticles. Nanomedicine: Nanotechnology, Biology, and Medicine, 2, 8– 21.
40. Barichello, J.M., Morishita, M., Takayama, K., Nagai, T., 1999. Encapsulation of hydrophilic and lipophilic drugs in PLGA nanoparticles by the nanoprecipitation method. Drug Dev Ind Pharm, 25, 471- 6.
41. Quintanar-Guerrero, D., Allemann, E., Fessi, H., Doelker, E., 1998. Preparation techniques and mechanism of formation of biodegradable nanoparticles from preformed polymers. Drug Dev Ind Pharm, 24, 1113-28.
42. Vauthier, C., Dubernet, C., Fattal, E., Pinto-Alphandary, C.P., 2003. Poly (alkylcyanoacrylates) as biodegradable materials for biomedical applications. Adv Drug Deliv Rev, 55, 519- 48.
43. Nagavarma, B.V.N., Yadav, H.K.S., Ayaz, A., Vasudha, L.S., Shivakumar, H.G., 2012. Different Techniques for Preparation of Polymeric Nanoparticles- A Review. Asian J Pharm Clin Res, 5, 16-23.
44. Jung, T., Kamm, W., Breitenbach, A., Kaiserling, E., Xiao, J.X., Kissel, T., 2000. Biodegradable nanoparticles for oral delivery of peptides: is there a role for polymers to affect mucosal uptake? Eur J Pharm Biopharm, 50, 147- 60.
45. Lambert, G., Fattal, E., Couvreur, P., 2001. Nanoparticulate system for the delivery of antisense oligonucleotides. Adv Drug Deliv Rev, 47, 99 – 112.
46. Couvreur, P., Dubernet, C., Puisieux, F., 1995. Controlled drug delivery with nanoparticles: current possibilities and future trends. Eur J Pharm Biopharm, 41, 2 - 13.
47. Sane, A., Thies, M.C., 2007. Effect of material properties and processing conditions on RESS of poly (l-lactide). J Supercrit Fluids, 40, 134–43.
48. Kreuter, J., 1982. The mechanism of termination in heterogeneous polymerization. J Polym Sci, 20, 543- 5.
49. Rao, J.P., Geckeler, K.E., 2011. Polymer nanoparticles: Preparation techniques and size control parameters. Progress in Polymer Science, Elsevier 36, 887-913.
50. Puig, J.E., 1996. Microemulsion polymerization (oil-in water). In: Salamone JC, editor. Polymeric materials encyclopedia, (6) Boca Raton, FL: CRC Press, 4333–41.
51. Gasco, M., Trotta, M., 1986. Nanoparticles from microemulsions. Int J Pharm1986, 29, 267–8.
52. Dustgania, A., Farahania, E.V., Imanib, M., 2008. Preparation of Chitosan Nanoparticles Loaded by Dexamethasone Sodium Phosphate. Iranian J Pharma Sci, 4, 111-114.

53. Redhead, H.M., Davis, S.S., Illum, L., 2001. Drug delivery in poly (lactide-coglycolide) nanoparticles surface modified with poloxamer 407 and poloxamine 908: in vitro characterisation and in vivo evaluation. J. Controlled Release 70, 353–363.
54. Betancor, L., Luckarift, H.R., 2008. Bioinspired enzyme encapsulation for biocatalysis. Trends in Biotechnology, 26, 566-572.
55. Ranjit, K., Baquee, A.A., 2013. Nanoparticle: An Overview of Preparation, Characterization and Application. Int. Res. J. Pharm. 4, 47-57.
56. Scholes, P.D., Coombes, A.G., Illum, L., Davis, S.S., Wats, J.F., Ustariz, C., Vert, M., Davies, M.C., 1999. Detection and determination of surface levels of polaxamer and PVA surfactant on biodegradable nanospheres using SSIMS and XPS. J. Control. Releae, 59, 261-278.
57. Singh, R., Lillard Jr, J.W., 2008. Nanoparticle-based targeted drug delivery. Exp. Mol. Pathol. 86, 215-223.
58. Magenheim, B., Levy, M.Y., Benita, S., 1993. A new in vitro technique for the evaluation of drug release profile from colloidal carriers-ultrafiltration technique at low pressure. Int. J. Pharm. 94, 115–123.
59. Fresta, M., Puglisi, G., Giammona, G., Cavallaro, G., Micali, N., Furneri, P.M., 1995. Pefloxacine mesilate- and ofloxacin-loaded polyethylcyanoacrylate nanoparticles: characterization of the colloidal drug carrier formulation. J. Pharm. Sci. 84, 895–902.
60. Shingai, M., Moses, O.O., 2009. Nanotechnology in Drug Development and Life Cycle Management. M.M. de Villiers et al. (eds.), Nanotechnology in Drug Delivery, Chapter 20, 597 – 619.
61. Lu, B., Zhang, J.Q., Yang, H., 2003. Lung-targeting microspheres of carboplatin. Int J Pharm, 265, 1–11.
62. Kreuter, J., 2001. Nanoparticulate systems for brain delivery of drugs. Adv. Drug Del. 47, 65-81.
63. Roy, I., Ohulchanskyy, T.Y., Pudavar, H.E., Bergey, E.J., Oseroff, A.R., Morgan, J., Dougherty, T.J., Prasad, P.N., 2003. Ceramic-based nanoparticles entrapping water-insoluble photosensitizing anticancer drugs: a novel drug-carrier system for photodynamic therapy. J Am Chem Soc. 125, 7860–7865.
64. Han, M., Gao, X., Su, J.Z., Nie, S., 2001. Quantum-dot-tagged microbeads for multiplexed optical coding of biomolecules. Nature Biotechnology. 19, 631–635.
65. Reich, D.H., Tanase, M., Hultgren, A., Bauer, L.A., Chen, C.S., Meyer, G.J., 2003. Biological applications of multifunctional magnetic nanowires. J Appl Phys. 93, 7275-7280.
66. Cao, Y.C., Jin, R., Nam, J.M., Thaxton, C.S., Mirkin, C.A., 2003. Raman dye-labeled nanoparticle probes for proteins. JACS. 125, 14676–14677.

Chapter - 2

Targeted Drug Delivery

TARGETED DRUG DELIVERY

Targeted drug delivery is an advanced method of delivering drugs to the patients in a site specific manner. The targeted drug delivery system increases the concentration of delivered drug to the targeted body part of interest only (organs/tissues/cells) which in turn improves efficacy of treatment by reducing side effects of drug administration. By means of targeted drug delivery system, drug of interest can be delivered in a certain amount for a prolonged period of time to a targeted diseased area within the body. This helps to maintain the required plasma and tissue drug levels in the body; therefore, avoiding any damage to the healthy tissue caused by the drug. Products based on such a delivery system are being prepared by considering the specific properties of target cells, nature of the markers or transport carriers or vehicles which convey drug to specific receptors, ligands and physically modulated components.

An ideal targeted drug delivery system should meet the following criteria [1, 2]:

- It should be biochemically inert (non-toxic) and non-immunogenic.
- It should be physically and chemically stable in vivo and in vitro conditions.
- It should have restricted drug distribution to target cells or tissues or organs and should have uniform capillary distribution.
- It should have controllable and predictable rate of drug release and also drug release should not affect the drug action.
- It should have therapeutic amount of drug release and should have minimal drug leakage during transit.

Targeted drug delivery system is preferred over conventional drug delivery systems due to three main reasons. The first being pharmaceutical reason. Conventional drugs have low solubility and more drug instability in comparison to targeted drug delivery systems. Conventional drugs also have poor absorption, shorter half-life and require large volume of distribution. These constitute its pharmacokinetic properties. The third reason constitutes the pharmacodynamic properties of drugs. The conventional drugs have low specificity and low therapeutic index as compared to targeted drug delivery system. Due to these reasons targeted drug delivery system is preferred over conventional drug delivery systems [3, 4].

2.1 Types of Targeted Drug Delivery:

Targeting drug to a specific area not only increases the therapeutic efficacy of drugs but also aims to decrease the toxicity associated with drug to allow lower doses of the drug to be used in therapy. For the fulfilment of such conditions, two approaches are used extensively:

a) Passive targeting: In passive drug targeting, the drug's success is directly related to circulation time [5]. This is achieved by cloaking the nanoparticle with some sort of coating. Several substances can achieve this, with one of them being polyethylene glycol (PEG). By adding PEG to the surface of the nanoparticle, it is rendered hydrophilic, thus allowing water molecules to bind to the oxygen molecules on PEG via hydrogen bonding. The result of the bonding is a film of hydration around the nanoparticle which makes the substance antiphagocytic. The particles obtain this property due to the hydrophobic interactions that are natural to the reticuloendothelial system (RES), thus the drug-loaded nanoparticle is able to stay in circulation for a longer period of time [6]. To work in conjunction with this mechanism of passive targeting, nanoparticles that are between 10 to 100 nanometers in size have been found to circulate systemically for longer periods of time [7].

b) Active targeting: Active targeting means a specific ligand-receptor type interaction for intracellular localization which occurs only after blood circulation and extravasations. This active targeting approach can be further classified into three different levels of targeting which are 1) First order targeting refers to restricted distribution of the drug carrier systems to the capillary bed of a predetermined target site, organ or tissue e.g. compartmental targeting in lymphatics, peritoneal cavity, plural cavity, cerebral ventricles and eyes, joints. 2) Second order targeting refers to selective delivery of drugs to specific cell types such as tumour cells and not to the normal cells e.g. selective drug delivery to kupffer cells in the liver. 3) Third order targeting refers to drug delivery specifically to the intracellular site of targeted cells e.g. receptor based ligand mediated entry of a drug complex into a cell by endocytosis [8]. By utilizing both passive and active targeting, a drug-loaded nanoparticle has a heightened advantage over a conventional drug. It is able to circulate throughout the body for an extended period of time until it is successfully attracted to its target through the use of cell-specific ligands, magnetic positioning, or pH responsive materials. Because of these advantages, side effects from conventional drugs will be largely reduced as a result of the drug-loaded nanoparticles affecting only diseased tissue [9].

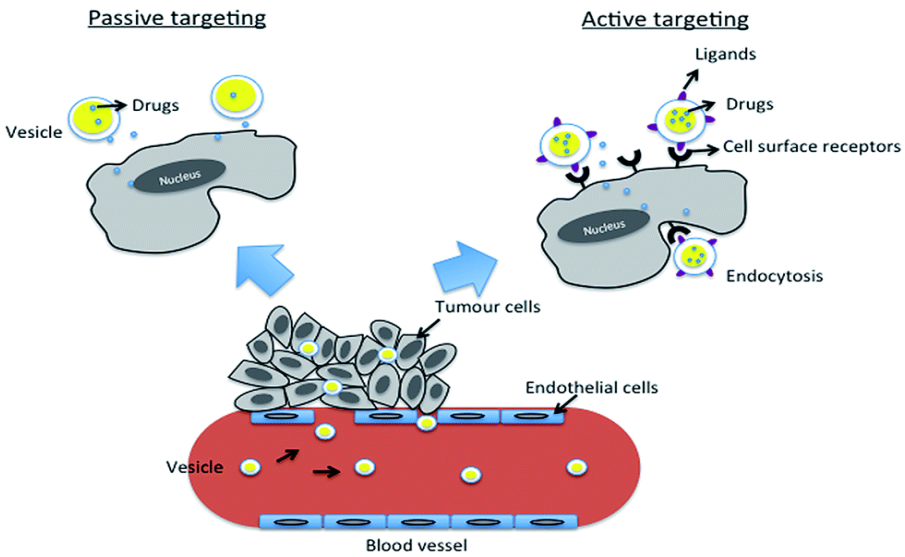

Fig 2.1 Schematic diagram of passive and active targeting [source: pubs.rsc.org]

REFERENCES

1. Mastrobattista, E., Koning, G.A., Storm, G., 1999. Immunoliposomes for the targeted delivery of antitumor drugs. Advance Drug Delivery Reviews, 10, 103-127.
2. Vyas, S.P., Khar, R.K., 2008. Basis of targeted Drug Delivery. In Targeted and controlled Drug Delivery, CBS Publishers and Distributors Reprint, 42-46, 74.
3. Muller, R.H., Keck, C.M., 2004. Challenges and solutions for the delivery of biotech drugs-a review of drug nanocrystal technology and lipid nanoparticles. J. Biotechnol. 113, 151-170.
4. Rani, K., Paliwal, S., 2014. A Review on Targeted Drug Delivery: its Entire Focus on Advanced Therapeutics and Diagnostics. Sch. J. App. Med. Sci., 2, 328-331.
5. Sagnella, S.; Drummond, C., 2012. Drug Delivery: A Nanomedicine Approach. Australian Biochemist, 43, 5–8, 20.
6. Vlerken, L.E.V., Vyas, T. K., Amiji, M.M., 2007. Poly (Ethylene Glycol)-Modified Nanocarriers for Tumor-Targeted and Intracellular Delivery. Pharm. Res. 24, 1405–1414.
7. Gullotti, E.; Yeo, Y., 2009. Extracellularly Activated Nanocarriers: A New Paradigm of Tumor Targeted Drug Delivery. Mol. Pharm., 6, 1041-1051.
8. Kannagi, R., Izawa, M., Koike, T., Miyazaki, K., Kimura, N., 2004. Carbohydrate-mediated cell adhesion in cancer metastasis and angiogenesis. Cancer Science, 95, 377-384.
9. Mitra, A. K., Kwatra, D., Vadlapudi, A.D., 2015. Drug Delivery; Jones & Bartlett Learning: Burlington, Massachusetts, 16, 1-9.

Chapter - 3

Use of Aptamers for Targeted Drug Delivery

USE OF APTAMERS FOR TARGETED DRUG DELIVERY

With the rapid development of nanotechnology, various nanostructured materials have been successfully synthesized for biomedical applications. The diverse characteristics with multifunctional capability of nanoparticles represent a promising potential in cancer therapy. These nanomaterials can nonspecifically accumulate in cancer tissue through the enhanced permeability and retention (EPR) effect. Conjugation of nanomaterials with targeting ligands that bind to overexpressed antigens or receptors on target cells has begun to represent a potentially powerful technology in cancer treatment. This specific binding to targeted cells leads to an increased accumulation of nanomaterials on target cells while minimizing harmful toxicity to non-target cells. Aptamers are one of such targeting ligands.

3.1 Aptamers:

Aptamers are short, synthetic, single-stranded oligonucleotides that specifically bind to various molecular targets, including small molecules, proteins, nucleic acids, and even cells and tissues with high affinity and specificity [1]. The term aptamer is derived from the Latin word "aptus"- which means fitting and the Greek word "meros" meaning particle. Compared with traditional ligands, including antibodies, peptides and small molecules, aptamers exhibit advantages such as low cost, low immunogenicity and toxicity, a small size to enable solid tumor penetration and high affinity to bind with the target, all of which make aptamers ideal candidates for targeted cancer therapy [2]. The most important property of an aptamer, is its high target selectivity. These short, chemically synthesized, single-stranded (ss) RNA or DNA oligonucleotides fold into specific three-dimensional (3D) structures with dissociation constants usually in the pico- to nano-molar range [3]. Moreover, in contrast to other nucleic acid molecular probes, aptamers interact with and bind to their targets through structural recognition, a process similar to that of an antigen-antibody reaction. Thus, aptamers are also referred to as "chemical antibodies."

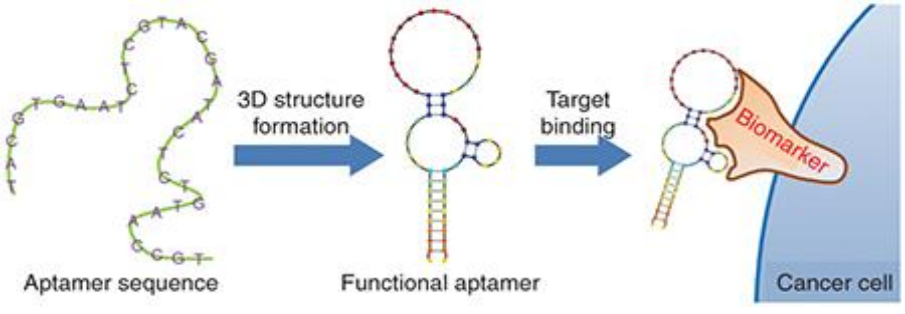

Fig 3.1 Schematic diagram of aptamer binding to its target [source: openi.nlm.nih.gov]

3.1.1 Structure and stability

Since single-stranded oligonucleotides follow the very same rules of complementarity of nucleic bases as do double-stranded molecules, it is relatively simple to predict their secondary structure. Numerous secondary motifs of aptamers have been described, including the **hairpin** structure, **pseudoknot** or the **G-quadruplex** [4].

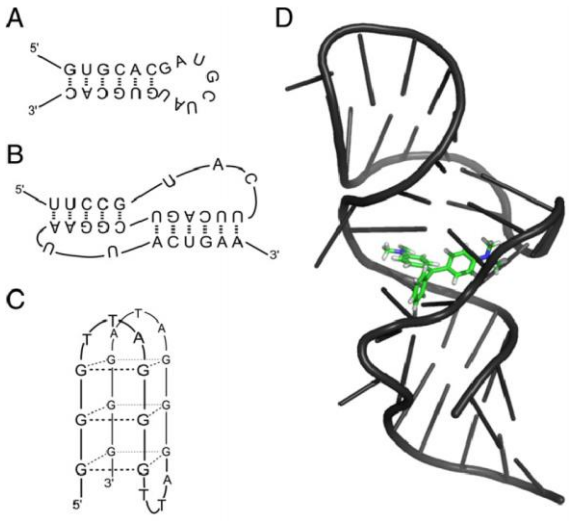

Fig 3.2 Aptamer structures. Schematic secondary structures of aptamer: hairpin (A), pseudoknot (B), G-quadruplex (C) and a three-dimensional representation of an anti-malachite green aptamer in complex with its ligand (D) Ref: Ranjan et al. 2016

Aptamers fold through intramolecular interaction to create tertiary conformations with specific binding pockets which bind to their target molecules with high specificity and affinity. Aptamers typically bind with an equilibrium dissociation constant (Kd) in the range of 10 pM to 10 μM [5] to a wide array of molecular targets [6] including other nucleic acids, proteins, peptides and small molecules. Aptamers can be described by a sequence of approximately 15 – 60 nucleotides (A, U, T, C, and G). The conformation of the aptamer confers specificity for a target molecule through interacting with multiple domains, or a binding pocket. Small changes in the target molecule can foil interactions and thus aptamers can distinguish between closely related but non-identical targets. For example, specific RNAs were identified. That have a high affinity for the bronchodilator theophylline (1,3-dimethylxanthine) yet exhibit a >10,000 times weaker binding affinity to caffeine (1, 3,7-trimethylxanthine) which differs from theophylline only by the substitution of a methyl group at the nitrogen atom N7 position [7]

The presence of a 2′-OH group and non-Watson-Crick base pairing allows RNA aptamer oligonucleotides to fold into more diverse 3D structures than ssDNA molecules. Consequently,

use of flexible RNA sequences simplifies the development of aptamers with high-affinity and specificity. Despite their advantages, RNA sequences are very sensitive to nucleases present in biological environments and are rapidly degraded [8]. To increase nuclease resistance of RNA-based aptamers, several chemical modifications have been investigated. Evidence shows that 2′-OH group and phosphodiester linkages of RNA sequences are the sites of nuclease hydrolysis. Subsequently, substitutions of the 2′-OH functional group by 2′-fluoro, 2′-amino, or 2′-O-methoxy motifs, and/or changes to the phosphodiester backbone with boranophosphate or phosphorothioate are the most common modifications aimed at increasing nuclease resistance [9]. More recently, Wu *et al*. developed a novel chemical modification method to increase siRNA stability, in which phosphorodithioate and 2′-O-methyl were simultaneously substituted in the same nucleotide [10]. This modification method significantly enhanced siRNA stability and represents a potential new direction for utilization of RNA-based therapies in complex biological systems. Other effective modifications recently reported utilizing the locked nucleic acid technology [11, 12] or generate "mirror" RNA sequence structures, termed spiegelmers [13]. These modifications result in structural changes to the RNA sequences, which cannot be digested by nucleases.

In addition to RNA aptamers, ssDNA-based aptamers have also been developed. Due to their lack of 2′-OH groups, DNA molecules are naturally resistant to 2′-endonucleases and are stable in biological environments.

3.1.2 Selection and synthesis

Aptamers are isolated using an iterative protocol called *in vitro* selection or *Systematic Evolution of Ligands by Exponential Enrichment* (SELEX), based on a repetitive amplification and enrichment process.

Starting point of a typical SELEX process is a chemically synthesized random DNA oligonucleotide library consisting of about 10^{13} to 10^{15} different sequence motifs [14]. In a SELEX procedure which is directed to the selection of DNA aptamers, this library can be used without any pretreatments, whereas a conversion into an RNA library has to accomplish prior starting an RNA SELEX process. In either case the randomized RNA or DNA pool is incubated directly with the target. The binding complexes are subsequently partitioned from unbound and weakly bound oligonucleotides. This is one of the most crucial aspects of an aptamer selection process and strongly affects binding features of the aptamers to be selected. Target bound oligonucleotides are eluted and amplified by PCR (DNA SELEX) or reverse transcription (RT)-PCR (RNA SELEX).

The resulting double-stranded DNA has to be transformed into a new oligonucleotide pool by separating the relevant ssDNA or by in vitro transcription and subsequent purifying the synthesized RNA. This new and enriched pool of selected oligonucleotides is used for a binding reaction with the target in the next SELEX round. By iterative cycles of selection and amplification the initial random oligonucleotide pool is reduced to relatively few sequence motifs with the highest affinity and specificity for the target. The number of rounds necessary depends on a variety of parameters, such as target features and concentration, design of the starting random DNA oligonucleotide library, selection conditions, ratio of target molecules to oligonucleotides, or the efficiency of the partitioning method. Additional steps can be introduced into each round of the SELEX process particularly with regard to the specificity of the oligonucleotides [15]. The detection of an enrichment of target-specific oligonucleotides indicates that the SELEX process is finished. The last SELEX round is stopped after the amplification step and the PCR products are cloned to get individual aptamer clones from the selected pool. These individual aptamers are sequenced and each sequence is analyzed. Representative aptamer clones are chosen and used in binding assays to characterize their binding features in more detail including the affinities and specificities. Mutation and truncation experiments can be performed to narrow down the minimal binding region within the aptamer sequence. Finally, most of the selected aptamers are subjected to some post-SELEX modifications, e.g. with the view to enhance the stability of the aptamers (incorporation of modified nucleotides), in order to use the aptamers in analytical detection assays or for target purification (attachment of reporter groups, functional groups or linker molecules) [14].

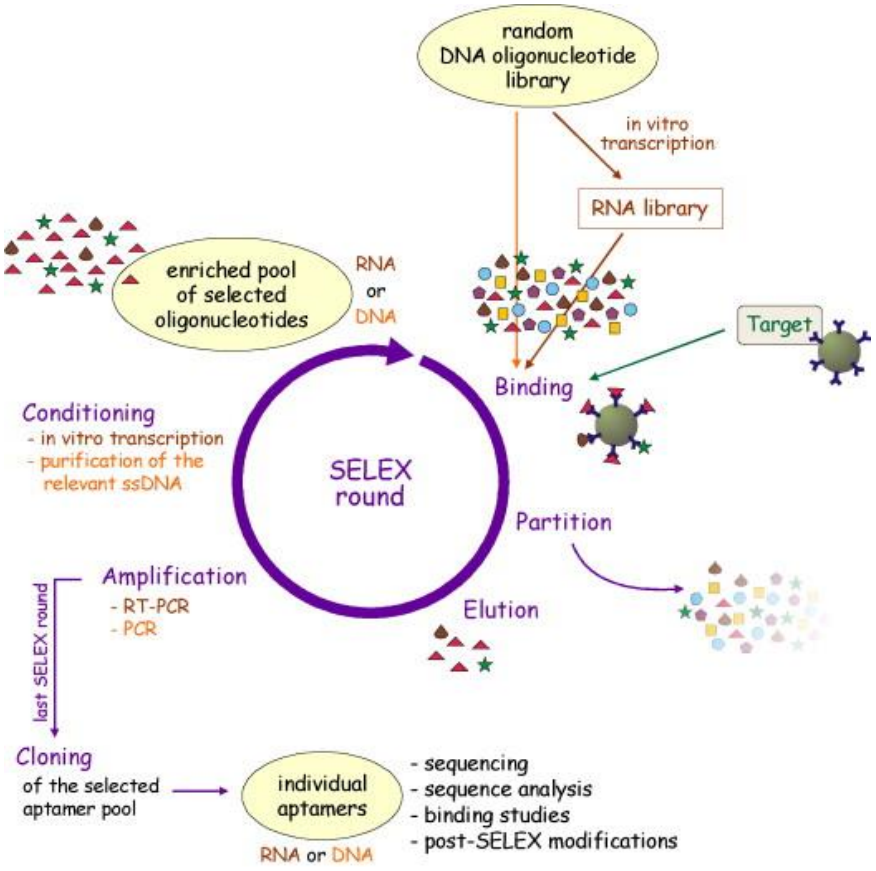

Fig 3.3 In vitro selection of target-specific aptamers using SELEX technology [Ref: Stoltenburg et al 2007]

3.2 Aptamer vs. Antibodies

Due to their small size and oligonucleotide properties, aptamers offer several advantages over protein antibodies in (i) their extensive clinical applicability and (ii) a less challenging industrial synthesis process. Some specific advantages of aptamer over antibodies are given below:

- Aptamers can penetrate tissues faster and more efficiently due to their significantly lower molecular weight (8–25 kDa aptamers versus ~150 kDa of antibodies).
- Aptamers are virtually nonimmunogenic *in vivo.*
- Aptamers are thermally stable. Based on the intrinsic property of oligonucleotides, even after a 95°C denaturation, aptamers can refold into their correct 3D conformations once cooled to room temperature. In comparison, protein-based antibodies permanently lose their activity at high temperatures.
- Rapid, large-scale aptamer synthesis and modification capacity that includes a variety of functional moieties.

- Low structural variation during chemical synthesis and have lower production costs.

3.3 Conjugation of nanoparticles to aptamers

Covalent conjugation of aptamers to substrates or drug delivery vehicles can be achieved most commonly through succinimidyl ester – amine chemistry which results in a stable amide likage [16, 17] or through maleimide – thiol chemistry. Potential noncovalent strategies include affinity interactions (i.e. streptavidan-biotin) and metal coordination (i.e. between polyhistidine tag at the end of the aptamer and Ni+2 chelates with immobilized nitrilotriacetic acid on the surface of the polymer particles). Covalently linked bioconjugates may result in enhanced stability in physiologic salt and pH while avoiding the unnecessary addition of biological components (i.e. streptavidin) thus minimizing immunologic reactions and potential toxicity. For covalent conjugation, the aptamer is typically modified to carry a terminal primary amine or thiol group which is in turn conjugated, respectively, to activated carboxylic acid N-hydroxysuccinimide (NHS) ester or maleimide functional groups present on the surface of drug delivery vehicles. These reactions are carried out under aqueous conditions with a product yield of 80 – 90% [18]. One potential difficulty with maleimide – thiol chemistry is the oxidation of the thiol group attached to aptamers during storage (formation of S – S bond between two thiol modified aptamers), resulting in dimers of aptamers which are not able to participate in the conjugation reaction with the malimide group on particles. This problem can be partially alleviate by using a reducing agent such as tris (2-carboxyethyl) phosphine (TCEP), betamercaptoethanol or dithiothreitol (DTT) during the conjugation reaction. Furthermore, a potential advantage of using NHS – amine chemistry is that the unreacted carboxylic acid groups on the particle surface make the particle surface charge (ζ potential) slightly negative thus, reducing non-specific interaction between the negatively charged aptamers and the negative particle surface. The conjugation of aptamers to nanoparticles can be qualitively confirmed by fluorescent microscopy or flow cytometry through the use of fluorescent probes, [such as fluorescein iso-thiocyanate (FITC)] that are conjugated directly to the aptamers or indirectly to complemantary oligonucleotides that hybridize to the aptamers [16]. Alternatively analytical approaches such as X-ray photoemission (XPS) may be used for characterization of the nanoparticle surface to confirm the extent of conjugation. The presence of a hydrocarbon spacer group between the nanoparticle surface and the aptamer should improve the probability of interaction between the aptamer and its target. Furthermore, a consistent density of the aptamer on

the surface of nanoparticles can potentially be achieved through utilizing an excess molar amount of aptamer relative to the reactive group on the nanoparticle surface during the conjugation reactions.

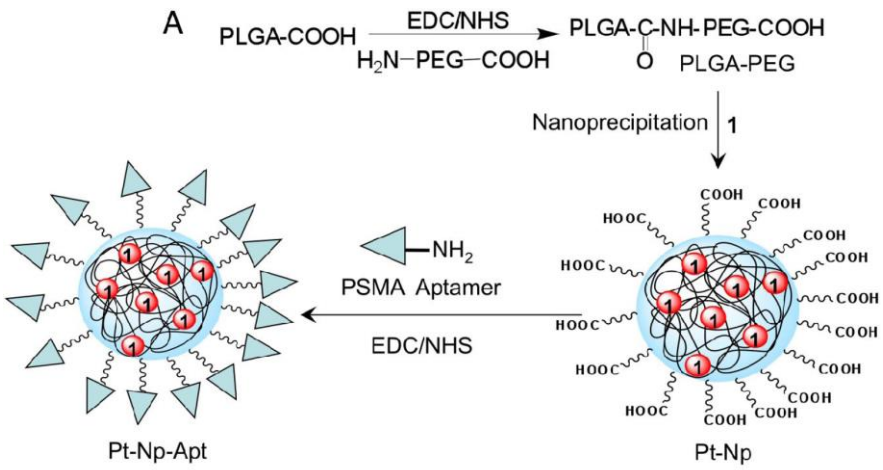

Fig 3.4 A summarized version of aptamer conjugation to PLGA nanoparticles with PEG used as a spacer molecule. The drug used was Cisplatin (Pt) denoted as 1. Both the NH2-PEG-COOH and anti-PSMA aptamer were conjugated to the PLGA molecule and the nanoparticle respectively using 1-ethyl-3-[3 dimethylaminopropyl] carbodiimide hydrochloride (EDC) and *N*-hydroxy succinimide (NHS), forming amide bonds.

LITERATURE REVIEW

Liu et al. designed and developed functional DNA nanostructures to deliver doxorubicin (Dox) to resistant cancer cells [19]. These nanostructures had two components. The first component was a DNA aptamer, which formed a dimeric G-quadruplex nanostructure to target cancer cells by binding with nucleolin**.** The second component was double-stranded DNA (dsDNA), which was rich in -GC- base pairs that could be applied for Dox delivery. They demonstrated that Dox was able to efficiently intercalate into dsDNA and this intercalation did not affect the aptamer's three-dimensional structure. In addition, the aptamer-dsDNA (ApS) nanoparticle showed good stability and protected the dsDNA from degradation in bovine serum. *In vivo* evaluation of this platform demonstrated potent antitumor efficacy and attenuated cardiotoxicity. The specific aptamer section recognized their targets with extraordinary affinity and selectively transported anticancer drug payload into target cancer cells to induce potent cytotoxicity, while dramatically reducing drug toxicity to other tissues. Besides doxorubicin, this platform can also be used to load other anticancer drugs (daunorubicin, cisplatin, *etc.*) with similar drug loading method as mentioned in the work, making it widely applicable as a promising drug delivery system candidate for targeted drug delivery.

Jalalian et al. evaluated Epirubicin-5TR1 aptamer–SPION tertiary complex for the imaging and treatment of murine colon carcinoma cells (C26 cells, target) [20]. For cytotoxic studies (MTT assay), they have treated the C26 and CHO-K1 (Chinese hamster ovary cells, nontarget) cells with either Epi or Epi–Apt–SPION tertiary complex. Internalization was evaluated by flow cytometry and Apt-SPION bioconjugate was used for imaging of cancer *in vivo*. Flow cytometric analysis showed that the tertiary complex was internalized effectively to C26 cells, but not to CHO-K1 cells. Cytotoxicity of Epi–Apt–SPION tertiary complex also confirmed internalization data. The complex was less cytotoxic in CHO-K1 cells when compared to Epi alone. No significant change in viability between Epi- and complex-treated C26 cells was observed. Magnetic resonance imaging (MRI) indicated a high level of accumulation of the nano-magnets within the tumor site. They have concluded that Epi–Apt–SPION tertiary complex is introduced as an effective system for targeted delivery of Epi to C26 cells.

Aravind et al. designed a multifunctional nanocarrier constructed from poly (D, l-lactide-co-glycolide) nanoparticles (PLGA NPs), an anticancer drug paclitaxel (PTX), a fluorescent dye Nile red (NR), magnetic fluid (MF) and aptamers (Apt, AS1411, anti-nucleolin aptamer) [21]. The magnetic fluid and paclitaxel loaded fluorescently labeled PLGA NPs (MF-PTX-NR-PLGA NPs) were synthesized by a single-emulsion technique/solvent evaporation method using a chemical cross linker bis (sulfosuccinimidyl) suberate (BS3) to enable binding of aptamer on to the surface of the nanoparticles. Targeting aptamers were then introduced to the particles through the reaction with the cross linker to target the nucleolin receptors expressed over on the cancer cell surface. Cytotoxicity assay conducted in two cell lines (L929 and MCF-7) confirmed that targeted MCF-7 cancer cells were killed while control cells were unharmed. In addition, aptamer mediated delivery resulting in enhanced binding and uptake to the target cancer cells exhibited increased therapeutic effect of the drug. Moreover, these aptamer conjugated magnetic polymer vehicles apart from actively transporting drugs into specifically targeted tumor regions can also be used to induce hyperthermia or for facilitating magnetic guiding of particles to the tumor regions.

Zhang et al. described a dual-functional mixed micellar system consisting of a pH-responsive copolymer D-α-tocopheryl polyethylene glycol 1000-blockpoly-(β-amino ester) (TPGS-b-PBAE, TP) and AS1411 aptamer (Apt) decorated TPGS polymer (Apt-TPGS), which recognizes the expressed over nucleolin on the plasma membrane of cancer cells [22]. The anti-cancer drug paclitaxel (PTX) was encapsulated in the Apt-mixed micelles, and these drug-loaded micelles had a suitable particle size and zeta potential of 116.3 nm ± 12.4 nm and −26.2 mV ±4.2 mV, respectively. Compared with non-Apt modified mixed micelles, more Apt-modified mixed micelles were internalized in SKOV3 ovarian cancer cells, whereas no significant difference in cellular uptake was observed in normal cells (LO2 cells). With a synergistic effect of cancer cell recognition and pH-sensitive drug release, significantly increased cytotoxicity and G2/M phase arrest against SKOV3 cells by PTX/Apt-mixed micelles were observed. Furthermore, intravenous administration of PTX/Apt-mixed micelles for 16 days significantly increased tumor accumulation of PTX, inhibited tumor growth, and reduced myelosuppression on tumor-bearing mice compared with free PTX injection. Therefore, this dual-functional Apt-mixed micellar system is a promising drug delivery system for targeted cancer therapy.

Bagalkot et al. produced physical aptamer-doxorubicin conjugates not requiring any chemical modification neither of the drug nor of the aptamer [23]. Doxorubicin (Dox) can intercalate into the aptamer portion. The authors studied *in vitro* binding and cell-specific uptake of the physical conjugates of the A10 PSMA aptamer by the PSMA-positive prostate cancer cell line LNCaP to evaluate the targeted drug delivery.

Farokhzad et al. reported docetaxel (Dtxl)-encapsulated nanoparticles formulated with biocompatible and biodegradable poly(D,L-lactic-*co*-glycolic acid)-*block*-poly(ethylene glycol) (PLGA-*b*-PEG) copolymer and surface functionalized with the A10 2'-fluoropyrimidine RNA aptamers that recognize the extracellular domain of the prostate-specific membrane antigen (PSMA), a well characterized antigen expressed on the surface of prostate cancer cells [24]. These Dtxl-encapsulated nanoparticle aptamer bioconjugates (Dtxl-NP-Apt) were shown binding to the PSMA protein expressed on the surface of LNCaP prostate epithelial cells and get taken up by these cells resulting in significantly enhanced *in vitro* cellular toxicity as compared with nontargeted nanoparticles that lack the PSMA aptamer (Dtxl-NP) and also exhibited remarkable efficacy and reduced toxicity as measured by mean body weight loss (BWL) *in vivo*.

Mann et al. developed long circulating liposomes with the outer surface decorated with thioated oligonucleotide aptamer (thioaptamer) against E-selectin (ESTA) and evaluated the targeting efficacy *in vitro* using Human Umbilical Cord Vein Endothelial Cell (HUVEC), demonstrating efficient and rapid uptake of the ESTA conjugated liposomes [25]. *In vivo*, the intravenous administration of ESTA-lip resulted in their accumulation at the tumor vasculature of breast tumor xenografts without shortening the circulation half-life.

Kang et al. successfully extended the application of aptamer-functionalized liposomes to the cellular level by incorporation of the cell-based aptamers and by simplification of the aptamer-modified liposome synthesis method using sgc8 aptamer. High binding affinity (Kd = 0.8 nM) toward leukemia CEM-CCRF cells, covalently linked the sgc8 aptamer to the liposome by PEG spacer [26].

Dhar et al. reported a unique strategy to deliver a lethal dose of cisplatin to prostate cancer cells by constructing Pt(IV) (*c,t,c*-[$Pt(NH_3)_2(O_2CCH_2CH2CH_2CH_2CH_3)_2Cl_2$])-encapsulated prostate-specific membrane antigen (PSMA) targeted nanoparticles (NPs) of poly(D,L-lactic-co-glycolic acid) PLGA-PEG-functionalized controlled release polymers coated with the PSMA aptamer A10 [27]. After cell-specific uptake of the Pt(IV)-NP-Apt bioconjugates, Pt(IV) was converted by cytosolic reduction processed into cisplatin. Cytotoxicity assays with LNCaP cells revealed a higher *in vitro* cytotoxic activity for the Pt(IV)-NP-Apt bioconjugates with respect to free cisplatin or bioconjugates lacking the aptamer portion.

Cheng et al. developed NPs from carboxyterminated poly (D,L-lactide-co-glycolide)- *block*-poly(ethylene glycol) (PLGA-*b*-PEG-COOH) polymer and studied the effects of altering various formulation parameters on the size of NPs. They conjugated the polymer to the A10 RNA aptamer (Apt) that binds to the Prostate Specific Membrane Antigen (PSMA) and evaluated in a LNCaP (PSMA+) xenograft mouse model of PCa. The surface functionalization of NPs with the A10 PSMA aptamer significantly enhanced delivery of NPs to tumors when the data were compared to those of nanoparticles without A10 PSMA aptamer [28].

REFERENCES

1. Fang, X., Tan, W., 2010. Aptamers generated from cell-SELEX for molecular medicine: a chemical biology approach. Acc. Chem. Res. 43, 48–57.
2. Zhang, Y., Hong, H., Cai, W., 2011. Tumor-targeted drug delivery with aptamers. Curr. Med. Chem. 18, 4185–4194.
3. Nimjee, S.M., Rusconi, C.P., Sullenger, B.A., 2005. Aptamers: an emerging class of therapeutics. Annu Rev Med 56, 555–583.
4. Ranjan A., Kumar S., Kumari R., Komal K., Kumar M., 2016. Aptamers: An Insight for Fisheries Research. J Aquac Mar Biol 4, 1-5.
5. Hermann, T., Patel, D.J., 2000. Adaptive recognition by nucleic acid aptamers. Science 287, 820-5.
6. Wilson, D. S., Szostak, J.W., 1999. In vitro selection of functional nucleic acids. Annu Rev Biochem 68, 611-47.
7. Jenison, R.D., Gill, S.C., Pardi, A., Polisky, B., 1994. High-resolution molecular discrimination by RNA. Science 263, 1425-9.
8. Soutschek, J., Akinc, A., Bramlage, B., Charisse, K., Constien, R., Donoghue, M et al. 2004. Therapeutic silencing of an endogenous gene by systemic administration of modified siRNAs. Nature 432, 173–178.
9. Keefe, A.D., Cload, S.T., 2008. SELEX with modified nucleotides. Curr Opin Chem Biol 12, 448–456.
10. Wu, S.Y., Yang, X., Gharpure, K.M., Hatakeyama, H., Egli, M., McGuire, M.H. et al. 2014. 2'-OMe-phosphorodithioate-modified siRNAs show increased loading into the RISC complex and enhanced anti-tumour activity. Nat Commun 5, 3459.
11. Schmidt, K.S., Borkowski, S., Kurreck, J., Stephens, A.W., Bald, R., Hecht, M. et al. 2004. Application of locked nucleic acids to improve aptamer in vivo stability and targeting function. Nucleic Acids Res 32, 5757–5765.
12. Förster, C., Zydek, M., Rothkegel, M., Wu, Z., Gallin, C., Geßner, R. et al. 2012. Properties of an LNA-modified ricin RNA aptamer. Biochem Biophys Res Commun 419, 60–65.
13. Hongguang S., Xun Z., Patrick YL., Roberto R.R., Wen T., Youli, Z., 2014. Oligonucleotide Aptamers: New Tools for Targeted Cancer Therapy. Mol Ther Nucleic Acids, 3, 1-14.
14. Stoltenburg, R., Reinemann, C., Strehlitz, B., 2007. SELEX-A (r)evolutionary method to generate high-affinity nucleic acid ligands. Biomolecular Engineering, 24, 381-403.
15. Marshall, K.A., Ellington, A.D., 2000. In vitro selection of RNA aptamers. Methods Enzymol. 318, 193–214.
16. Farokhzad, O.C., Jon, S., Khademhosseini, A., Tran, T.N., Lavan, D.A., Langer, R., 2004. Nanoparticle-aptamer bioconjugates: a new approach for targeting prostate cancer cells. Cancer Res 64, 7668-72.
17. Farokhzad, O.C., Khademhosseini, A., Jon, S., Hermmann, A., Cheng, J., Chin, C., Kiselyuk, A., Teply, B., Eng, G., Langer, R., 2005. Microfluidic system for studying the interaction of nanoparticles and microparticles with cells. Anal Chem 77, 5453-9.
18. Sehgal, D., Vijay, I.K., 1994. A method for the high efficiency of water-soluble carbodiimide-mediated amidation. Anal Biochem 218, 87-91.

19. Liu, J., Tuo, W., Jing, Z., Yuanyu, H., Hua, D., Kumar, A., Chenxuan, W., Zicai, L., Xiaowei, M., Xing-Jie, L., 2014. Multifunctional Aptamer-based Nanoparticles for Targeted Drug Delivery to Circumvent Cancer Resistance. Nano Lett. 14, 2843-2848.
20. Jalalian, S.H., Taghdisi, S.M., Hamedani, N.S., Kalat, S.A.M., Lavaee, P. et al. 2013. Epirubicin loaded super paramagnetic iron oxide nanoparticle-aptamer bioconjugate for combined colon cancer therapy and imaging in vivo. Eur. J. Pharm. Sci. 50, 191–197.
21. Aravind, A., Nair, R., Raveendran, S., Veeranarayanan, S., Nagaoka, Y., Fukuda, T. et al. 2013. Aptamer conjugated paclitaxel and magnetic fluid loaded fluorescently tagged PLGA nanoparticles for targeted cancer therapy. J. Magn. Magn. Mater. 344, 116-123.
22. Zhang, J., Chen, R., Fang, X., Chen, F., Wang, Y., Chen, M., 2015. Nucleolin targeting AS1411 aptamer modified pH-sensitive micelles for enhanced delivery and antitumor efficacy of paclitaxel. Nano Res. 8, 201-218.
23. Bagalkot, V., Farokhzad, O.C., Langer, R., Jon, S., 2006. An aptamer-doxorubicin physical conjugate as a novel targeted drug-delivery platform. Angewandte Chemie International Edition, 45, 8149–8152.
24. Farokhzad, O.C., Cheng, J., Teply, B.A., Sherifi, I., Jon, S., Kantoff, P.W., Richie, J.P., Langer, R., 2006. Targeted nanoparticle-aptamer bioconjugates for cancer chemotherapy in vivo. Proc. Natl. Acad. Sci. USA, 103, 6315–6320.
25. Mann, A.P., Bhavane, R.C., Somasunderam, A., Liz, M.O.B., Ghaghada, K.B., Volk, D., Nieves-Alicea, R., Suh, K.S., Ferrari, M., Annapragada, A., Gorenstein, D.G., Tanaka, T., 2011. Thioaptamer conjugated liposomes for tumor vasculature targeting. Oncotarget. 2, 298-304.
26. Kang, H.Z., O'Donoghue, M.B., Liu, H.P., Tan, W.H., 2010. A Liposome-based Nanostructure for Aptamer Directed Delivery. Chem. Commun. 46, 249–251.
27. Dhar, S., Gu, F.X., Langer, R., Farokhzad, O.C., Lippard, S.J., 2008. Targeted delivery of cisplatin to prostate cancer cells by aptamer functionalized Pt(IV) prodrug-PLGA-PEG nanoparticles. Proc. Natl. Acad. Sci. USA, 105, 17356–17361.
28. Cheng, J., Teply, B.A., Sherifi, I., Sung, J., Luther, G., Gu, F.X., Levy-Nissenbaum, E., Radovic-Moreno, A.F., Langer, R., Farokhzad, O.C., 2007. Formulation of Functionalized PLGA-PEG Nanoparticles for In Vivo Targeted Drug Delivery. Biomaterials, 28, 869–876.

Chapter - 4

OBJECTIVES

The aim of this research work was to develop and characterize a biodegradable nanoparticulate drug delivery system, using an anticancer drug Doxorubicin with the carboxylic acid terminated polymer PLGA (50:50). Further the best formulation was conjugated with aptamer for targeting of Mucin-1.

Different formulations were prepared by varying some formulation parameters such as emulsifier content, pH, modification of the aqueous medium, drug and polymer ratio etc. The optimized nanoparticle formulation was investigated and characterized for the following parameters:

- Drug-excipient interaction study by FTIR.
- Particle size and size distribution.
- Zeta potential and polydispersity index.
- Morphological characterization of nanoparticles.
- Drug loading study and loading efficiency.
- *In vitro* drug release study.

The next objective of the work was the chemical conjugation of single-strand modified DNA (ssDNA) aptamers to the surface of the optimized nanoparticle formulation. The single-strand modified DNA aptamers were designed to have affinity towards **Mucin- 1** (MUC1), also known as **polymorphic epithelial mucin** (PEM**),** a cell surface associated mucin glycoprotein. MUC-1 is overexpressed in epithelial sarcomas, adenocarcinoma, multiple myeloma and other types of neoplastic growths associated with blood, colon, breast, ovarian, lung and pancreatic cancers. Overexpression of the MUC-1 creates a highly hydrophilic region which prevents hydrophobic chemotherapeutic drugs from passing through. This prevents the drugs from reaching their targets which usually reside within the cell. MUC1 also prevents the interaction of immune cells with receptors on the cancer cell surface through steric hindrance. Association of MUC1 with p53 in cancer also results in inhibition of p53-mediated apoptosis and promotion of p53-mediated cell cycle arrest. Thus an aptamers targeting this receptor may facilitate better attachment of the nanoparticles containing chemotherapeutics to the tumor sites and hence enhance drug availability and reduce non-specific side-effects related to the therapy. The surface conjugation of the aptamers to the nanoparticles involves the carbodiimide linkage chemistry. The success of the conjugation will be verified through the agarose gel electrophoresis of the conjugated and non-conjugated nanoparticles along with the free DNA aptamer.

Chapter - 5

MATERIALS

NAME OF CHEMICALS	SOURCE
Doxorubicin (Dox)	Sun Pharma Pvt. Ltd, Mumbai, India
Poly (d,l-lactide-co glycolide) (PLGA) (50:50), acid terminated	Sigma Aldrich Chemicals PVT. LTD. Bangalore, India
Polyvinyl alcohol (PVA)	S.D. fine chem. Ltd. Mumbai, India
Dichloromethane (DCM)	Merck Specialties Pvt. Ltd. Mumbai, India
Ethidium bromide	Sigma Aldrich Chemicals PVT. LTD. Bangalore, India
Sodium chloride	Merck Specialties Pvt. Ltd. Mumbai, India
Disodium hydrogen orthophosphate	Merck Specialties Pvt. Ltd. Mumbai, India
Potassium hydrogen phosphate	Merck Specialties Pvt. Ltd. Mumbai, India
Sodium hydroxide	Merck Specialties Pvt. Ltd. Mumbai, India
Dimethyl sulfoxide (DMSO)	Merck Specialties Pvt. Ltd. Mumbai, India
Hydrochloric acid (35%) (HCl)	Merck Specialties Pvt. Ltd. Mumbai, India
Acetic acid (Glacial)	Merck Specialties Pvt. Ltd. Mumbai, India
1-Ethyl-3-(3-dimethylaminopropyl) carbodiimide hydrochloride (EDC)	HiMedia Laboratories Pvt. Ltd. Mumbai, India
N-Hydrosuccinimide (NHS)	HiMedia Laboratories Pvt. Ltd. Mumbai, India
Tris buffer, A.R.	HiMedia Laboratories Pvt. Ltd. Mumbai, India
Agarose, DNA grade (Low Melting)	HiMedia Laboratories Pvt. Ltd. Mumbai, India
Ethylene diamine tetra acetic acid (EDTA), sodium salt	Sisco Research Laboratories Pvt. Ltd. Mumbai, India
100 bp DNA Ladder	HiMedia Laboratories Pvt. Ltd. Mumbai, India
Aptamer S2.2 with spacer, 5'-GCA GTT GAT CCT TTG GAT ACC CTG GTT CCC TTC CTT CTC TCT TCC TCT CTC CTT CTC TCT TCC TCT CTC CTT C-3', with 3'-NH2 tail modification (HPLC purified)	M/S K.R. Instruments and Chemicals, Kolkata & Eurofins Genomics, Bangalore, India

EQUIPMENTS

EQUIPMENT	SOURCE
Advanced Microprocessor UV-VIS single beam Spectrophotometer (Model Intech-295)	Model Intech-295, Gentaur GmbH, Aachen, Germany
High speed homogenizer (Ultra-Turrax, model T10B)	IKA Laboratory Equipment, Staufen, Germany
Bath sonicator	Trans-O-Sonic, Mumbai, India
Lyophilizer	Indian Instruments and chemicals, Kolkata, India
Micro centrifuge (SPINWIN)	Lab equipments and chemicals, Kolkata, India
Cold-centrifuge	3k30 Sigma Lab Centrifuge, Merrington Hall Farm, Shrewsbury, UK
Incubator shaker	Indian Instruments and chemicals, Kolkata, India
FT-IR	Alpha, Bruker Alpha, Ettlingen, Germany
Gel electrophoresis chamber	Lab equipments and chemicals, Kolkata, India
Magnetic stirrer	Remi Equipments, Mumbai, India
Zeta sizer Nano ZS 90	Malvern Instrument Ltd. Malvern, UK
Scanning electron microscope	Zeiss instruments, Switzerland
Field Emission Scanning Electron Microscope	JEOL JSM 6700 F, JEOL, Tokyo, Japan

SPECIAL MATERIALS USED:

- **DOXORUBICIN:**

  Formula: $C_{27}H_{29}NO_{11}$

  Molecular mass: 543.52 g/mol

  IUPAC Name: (7S,9S)-7-[(2R,4S,5S,6S)-4- amino-5-hydroxy-6-methyloxan-2-yl]oxy-6,9,11-trihydroxy-9-(2-hydroxyacetyl)-4-methoxy-8,10-dihydro-7H-tetracene-5,12- dione

  Physical Nature: Red amorphous powder.

  Use: As a model chemotherapeutic agent to be encapsulated in the nanoparticles.

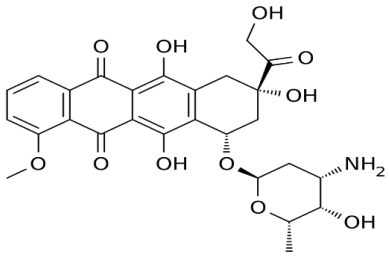

Fig 5.1 Structure of Doxorubicin

- **PLGA [Poly (d,l-lactide-co glycolide) (50:50), acid terminated]:**

  Formula: $[C_3H_4O_2]x\ [C_2H_2O_2]y$; $C_3H_4O_2$= Lactic acid, $C_2H_2O_2$= Glycolic acid.

  Feed ratio: Lactide: Glycolide = 50:50

  Molecular weight: 24,000-38000

  Physical nature: White, amorphous flakes.

  Use: As a polymer.

  Description: PLGA or poly (d,l-lactic-coglycolic acid) is a copolymer of two monomers poly lactic acid (PLA) and poly glycolic acid (PGA). During polymerization, successive monomeric units (of glycolic or lactic acid) are linked together in PLGA by ester linkages, thus yielding a linear, aliphatic polyester as a product [1]. Depending on the ratio of lactide to glycolide used for the polymerization, different forms of PLGA can be obtained: these are usually identified with regard to the molar ratio of the monomers used ((e.g. PLGA 50:50 identifies a copolymer whose composition is 50% lactic acid and 50% glycolic acid.). The crystallinity of PLGAs will vary from fully amorphous to fully crystalline depending on block structure and molar ratio.

  PLGA has been successful as a biodegradable polymer because it undergoes hydrolysis in the body to produce the original monomers, lactic acid and glycolic acid. Since the body effectively deals with the two monomers, there is minimal systemic toxicity associated with using PLGA for drug delivery or biomaterial applications. Also, the possibility to tailor the polymer degradation time by altering the ratio of the monomers used during synthesis has made PLGA a common choice in the production of a variety of biomedical devices, such as, grafts, sutures, implants, prosthetic devices, surgical sealant films, micro and nanoparticles [2]. The acid terminated species of PLGA has a free carboxylic acid moiety at the end of the polymer chain which can be chemically modified for conjugation purpose. Other modifications include ester termination which increases the shelf-life of the polymer by inhibiting hydrolysis.

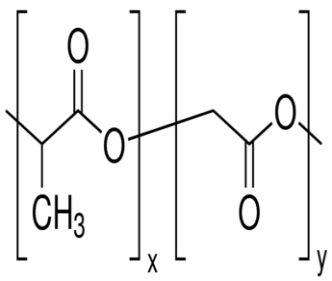

Fig 5.2 Structure of PLGA, x denotes no. of Lactide units (left); y denotes no. of Glycolide units (right).

- **Polyvinyl Alcohol (PVA):**

  Formula: $(C_2H_4O)n$

  Molecular Weight: 85,000-1, 24,000

  Description: Polyvinyl alcohol (PVA) is a water-soluble synthetic polymer. It is used mainly as a viscosity inducer, film forming agent and an ingredient in synthetic adhesives.

  Physical nature: White, odorless, crystalline beads.

  Use: As a viscosity enhancer and emulsifying agent in the aqueous phase for the emulsification process.

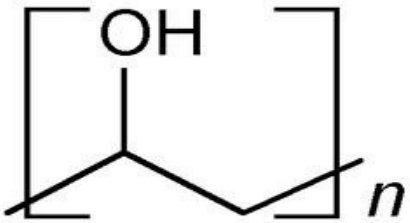

Fig 5.3 Structure of Polyvinyl Alcohol

- **S2.2 aptamer with spacer:**

Fig 5.4 The possible secondary structure of the S2.2 MUC-1 targeting aptamers with a spacer tail (Ref. - openi.nlm.nih.gov)

S2.2 is a DNA aptamers designed for targeting the MUC-1 glycoprotein receptor that are overexpressed (at least 10 folds) in various tumor cells including most malignant adenocarcinomas[3] like ovarian, lung, pancreatic and prostate cancers, as well as in primary and metastatic breast cancers [4]. The S2.2 is a 25 mer long oligonucleotide bearing the sequence 5'-GCA GTT GAT CCT TTG GAT ACC CTG G-3'. The spacer molecule was designed by Yu et al [4] to replace the conventional polyethylene glycol spacer molecule which functions in distancing the aptamers from the nanoparticle surface to facilitate polyvalent bindng of the nanocarrier with the target receptor [5].

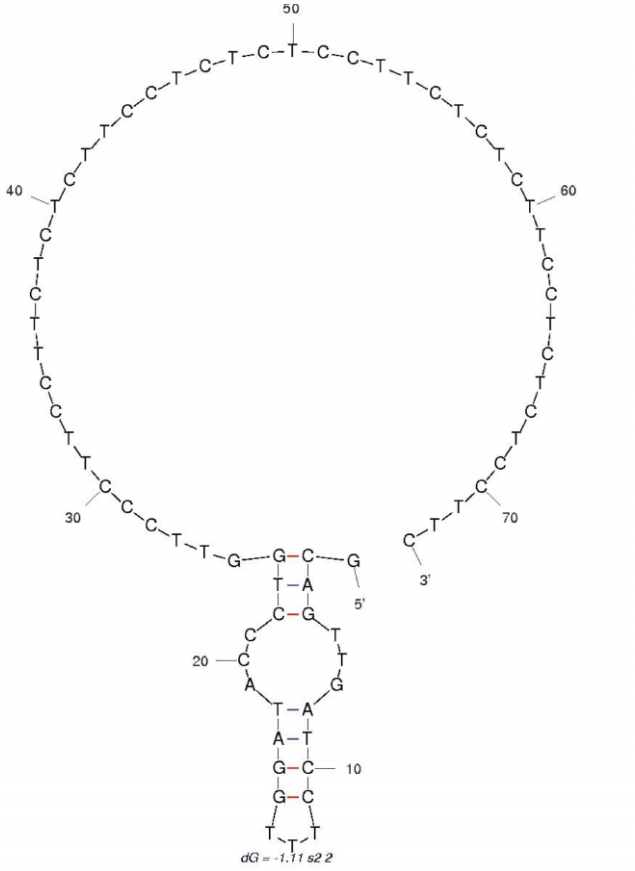

Fig 5.5 The folded structure of the S2.2 aptamer given by the mfold software [http://www.bioinfo.rpi.edu/applications/mfold/]. ΔG=-1.11 kcal/mol.

The 48 base long spacer is approximately 25 nm long which is near to the chain length of PEG 3400, the most commonly used spacer. Avoiding the PEG simplifies the preparation, bypassing the step required for chemical conjugation of the PEG molecule to PLGA and again the conjugation of the aptamer to the PEG and requiring only the conjugation of the aptamer with the PLGA nanoparticles. The aptamer is attached to a NH_2 terminal so that it can be conjugated with the free carboxyl groups of the PLGA to form peptide (amide) linkage through carbodiimide chemistry [4].

Sequence: 5'-GCA GTT GAT CCT TTG GAT ACC CTG GTT CCC TTC CTT CTC TCT TCC TCT CTC CTT CTC TCT TCC TCT CTC CTT C-3'

Modifications: NH_2 terminal at the 3'

Mol. Wt: 21905.2

- **1-Ethyl-3-(3-dimethylaminopropyl) carbodiimide hydrochloride (EDC):**

  IUPAC Name: 3-(Ethyliminomethyleneamino)-N, N-dimethylpropan-1-amine.

  Formula: $C_8H_{17}N_3$

  Mol. Wt.: 155.24 g/mol

  Description: EDC is a water-soluble carbodiimide usually obtained as the hydrochloride. It is typically employed in the 4.0-6.0 pH range. It is generally used as a carboxyl activating agent for the coupling of primary amines to yield amide bonds. Additionally, EDC can also be used to activate phosphate groups in order to form phosphomono-esters and phosphodiesters. Common uses for this carbodiimide include peptide synthesis, protein crosslinking to nucleic acids, but also in the preparation of immunoconjugates. EDC is often used in combination with *N*-hydroxysuccinimide (NHS) for the immobilisation of large biomolecules.

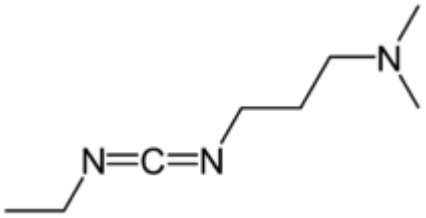

Fig. 5.6 Structure of EDC

  Use: As the conjugating agent between the PLGA nanoparticles and the NH_2 terminated aptamer.

- **N-Hydrosuccunimide (NHS):**

  IUPAC Name: 1-Hydroxy-2, 5-pyrrolidinedione

  Formula: $C_4H_5NO_3$

  Mol. wt.: 115.09 g/mol

  Description: NHS is commonly found in organic chemistry or biochemistry where it is used as an activating reagent for carboxylic acids. Activated acids (basically esters with a good leaving group) can react with amines to form amides for example, whereas a normal carboxylic acid would just form a salt with an amine. Often used in conjunction with EDC.

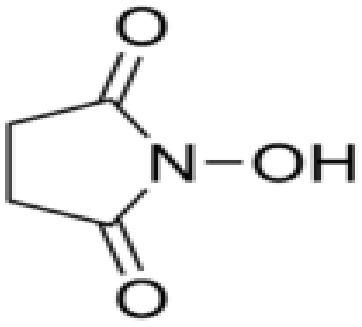

Fig 5.7 Structure of NHS

Use: As the conjugating agent between the PLGA nanoparticles and the NH_2 terminated aptamer.

- **Tris [tris(hydroxymethyl)aminomethane]:**

  IUPAC Name: 2-Amino-2-hydroxymethyl-propane-1, 3-diol

  Formula: $(HOCH_2)_3CNH_2$

  Mol. Wt.: 121.14 g/mol

  Description: Tris is an organic base which is used as a component of buffer solutions, such as in TAE (with acetic acid) and TBE (with boric acid) buffer, especially for solutions of nucleic acids.

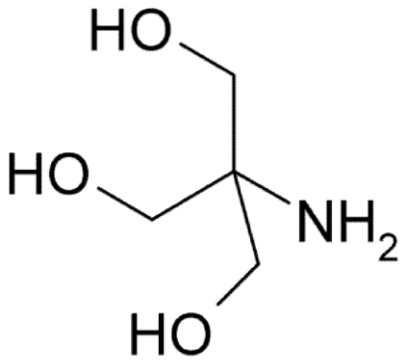

Fig 5.8 Structure of Tris.

Use: As a component of the TAE buffer system required for gel electrophoresis**.**

- **Ethidium Bromide:**

  IUPAC Name: 3, 8-Diamino-5-ethyl-6-phenylphenanthridinium bromide

  Formula: $C_{21}H_{20}N_3Br$

  Mol. Wt.: 394.29 g/mol

  Description: Ethidium bromide is an intercalating agent commonly used as a fluorescent tag (nucleic acid stain) for techniques such as agarose gel electrophoresis. When exposed to ultraviolet light, it will fluoresce with an orange colour, intensifying almost 20-fold after binding to DNA.

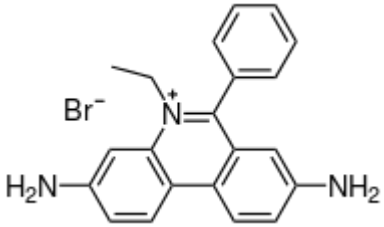

Fig 5.9 Structure of Ethidium Bromide

Use: As a stain for the nucleic acid during gel electrophoresis.

REFERENCES

1. Astete, C. E., Sabliov, C. M., 2006. "Synthesis and characterization of PLGA nanoparticles". Journal of Biomaterials Science – Polymer, 17, 247–289.
2. Pavot, V., Berthet, M., Rességuier, J., Legaz, S., Handké, N., Gilbert, S.C., Paul, S., Verrier, B., 2014. "Poly (lactic acid) and poly (lactic-co-glycolic acid) particles as versatile carrier platforms for vaccine delivery." Nanomedicine (London, England), 9, 2703–18.
3. Taylor-Papadimitriou, J., Burchell, J., Miles, D.W., Dalziel, M., 1999. MUC1 and cancer. BBA-Mol Basis Dis 1455, 301–313.
4. Yu, C., Hu, Y., Duan J., Yuan, W., Wang, C., et al. 2011. Novel Aptamer-Nanoparticle Bioconjugates Enhances Delivery of Anticancer Drug to MUC1-Positive Cancer Cells In Vitro. PLoS ONE 6, e24077.
5. Lee, R.J., Low, P.S., 1994. Delivery of liposomes into cultured KB cells via folate receptor mediated endocytosis. J Biol Chem 269, 3198–3204.

Chapter - 6

METHODOLOGIES

1.1 Development of Calibration Curves:

1.1.1 Determination of absorption maxima (λmax) of Doxorubicin:

For the determination of absorption maxima, Doxorubicin (Dox) was dissolved in dimethyl sulfoxide (DMSO) and phosphate buffer saline (PBS) pH 7.4 and scanned in the range of 190-600 nm using spectrophotometer. Two distinct λmax values were found at 259 and 480 nm in DMSO solution and a characteristic peak was found at 480 nm in PBS solution of doxorubicin, which were close to the published λmax of Doxorubicin. For the calculation purpose, the λmax of 480 nm was chosen.

1.1.2 Preparation of phosphate buffer saline (PBS) pH 7.40:

The release of the drug from nanoparticles was carried out in phosphate buffer saline (pH 7.4). To prepare phosphate buffer saline solution, disodium hydrogen orthophosphate (2.38 g), potassium dihydrogen orthophosphate (0.19 g) and sodium chloride (8 g) were dissolved in sufficient double distilled water (DDW) to produce 1000 mL and pH was adjusted to 7.4.

1.1.3 Preparation of calibration curves:

Two separate calibration curves were prepared- one in DMSO for calculation of drug loaded into nanoparticles and another in PBS for studying the release of drug from the nanoparticles. Three stock solutions of Dox were prepared by dissolving 30 mg of drug with successive dilution in volumetric flasks containing DMSO and PBS respectively. Final concentration of the stock solutions were made to 10μg/ml. From that stock solution, different concentrations were prepared – 1 μg/ml, 2 μg/ml, 4 μg/ml, 5 μg/ml, 6 μg/ml, 7 μg/ml, 8 μg/ml and 10 μg/ml for DMSO and 1 μg/ml, 2 μg/ml, 4 μg/ml, 5 μg/ml, 8 μg/ml and 10 μg/ml for PBS. The respective absorbance were read with three replicates using DMSO and PBS pH 7.4 as blank at 480nm using UV-Vis spectrophotometer. Calibration curves were drawn by plotting respective average absorbance against concentrations.

1.2 Preparation of Nanoparticles:

Double emulsification-solvent evaporation method was used for preparation of nanoparticles. Briefly, the method employs formation of primary emulsion and a secondary emulsion, followed

by sonication and solvent evaporation. Then the solidified nanoparticles were settled from the suspended state through centrifugation and freeze-dried for storage. The primary emulsion was prepared as a w/o type emulsion. Since doxorubicin is hydrophilic in nature, the drug was added in this aqueous phase. The aqueous phase was prepared by taking 0.5 ml of 2.5 % PVA solution in water and dissolving 5 mg of Dox in it. The hydrophobic or oil phase was prepared by dissolving 50 mg PLGA 50:50 (acid terminated) in 3ml of DCM. The aqueous phase was added drop by drop into the oil phase under high speed homogenization (x25,000rpm) and then the homogenization was continued for 10 minutes or till a cream like emulsion forms.. Then, the formed w/o emulsion was added drop wise into 50 ml of 1.5 % PVA solution in water under homogenization again to form a fine w/o/w emulsion. The final emulsion was sonicated with ice for 30 minutes in a bath sonicator. Then it was kept in the open with gentle stirring overnight for the evaporation of the volatile solvent. The final product after evaporation was centrifuged at around 2600 rcf (5000 rpm in Sigma Cooling Centrifuge) to settle out the microparticles. The precipitate was discarded and the supernatant was again centrifuged at around 26000 rcf (16000 rpm in Sigma Cooling Centrifuge) for 30 minutes to settle the nanoparticles. The settled nanoparticles were washed three times with double distilled water. The final product, in its slurry form, was frozen overnight and then lyophilized for 10 hours at -40˚C under vacuum to obtain completely freeze-dried nanoparticles.

Table 6.1 Different formulations that were prepared:

Formulation Code	Amount of Drug taken (mg)	Amount of PLGA taken (mg)	Conc. of inner PVA solution (%w/v)	Conc. of outer PVA solution (%w/v)	Nature of aqueous medium
F1	5	50	2.0	1	H_2O
F2	5	50	2.5	1.5	PBS (pH7.4)
F3	5	50	3.0	1.5	H_2O
F4	5	50	2.5	1.5	PBS(pH8)

1.3 Evaluation and characterization of Doxorubicin nanoparticles

1.3.1 Study of drug-excipients interaction through FT - IR spectroscopy:

Fourier transform infrared spectroscopy (**FTIR**) technique was used to study the drug-excipients interaction. Doxorubicin, PLGA, PVA, nanoparticles and the physical mixture of drug with PLGA

and PVA were prepared separately and scanned over a wave number range of 4000 to 400 cm^{-1} in a FT-IR instrument (**Bruker FTIR, TENSOR 27**). The obtained spectrophotograms were then interpreted for the functional groups present.

1.3.2 Study of morphology of nanoparticles by Scanning Electron Microscope (SEM):

The external morphology of nanoparticles of different formulations was analyzed by scanning electron microscopy. The freeze-dried particles were spread on to metal stubs and gold coating was done by using ion-sputtering device. These coated particles were then examined under the scanning electron microscope (Zeiss, Switzerland).

1.3.3 Morphological study by Field Emission Scanning Electron Microscope (FESEM):

After getting SEM data, freeze dried formulations (F2 & F4) were further processed for FESEM study to define the morphological characteristics of nanoparticles more accurately. The freeze dried particles were spread on the slide and examined under field emission scanning electron microscope (Zeiss, Switzerland).

1.3.4 Determination of size distribution, polydispersity index (PDI) and zeta potential:

To determine the size distribution, polydispersity index (PDI) and zeta potential, the prepared freeze-dried formulations were suspended in double distilled water and then poured into glass cuvette and analyzed by the instrument Zetasizer nano ZS (0.6 nm to 6000 nm) using DTS software V 4.0 (Malvern instrument Limited, Worcestshire, UK). For particle size measurement it uses dynamic light scattering (DLS) principle. The mean particle diameter was calculated by the software from the size distributions measured, Zeta potential of the particle surfaces and the polydispersity index (PDI) calculated was the measure of the size ranges of particles present in the suspension.

1.4 Drug Content and Entrapment Efficiency Study:

Dimethyl sulfoxide (DMSO), which is a common solvent for both PLGA and DOX was used to determine the drug content and entrapment efficiency of the prepared nanoparticles. 2 mg of each nanoparticle sample was taken in Eppendorf tube of 2 ml volume and dissolved in DMSO. Blank product (prepared without the drug) (2 mg) was dissolved in 2ml of DMSO. Then the solution with the blank nanoparticles was scanned in UV spectroscope (Advanced Microprocessor UV-VIS

single beam, Intech 295, USA) at 480 nm and set as blank or zero.Then the absorbance of the solution with the drug-loaded nanoparticles was measured for determining the content of doxorubicin in the prepared nanoparticles.

The drugloading (Theoretical and Practical) and entrapment efficiency were calculated by usingthe following formulae:

$$\% \text{ Drug loading (theoretical)} = \frac{\text{Amount of drug taken to prepare nanoparticles}}{\text{Amount of PLGA + Drug Taken}} \times 100$$

$$\% \text{ Drug loading (practical)} = \frac{\text{Amount of drug in nanoparticles}}{\text{Amount of nanoparticles obtained}} \times 100$$

$$\% \text{ Drug entrapment efficiency} = \frac{\% \text{ Drug loading (practical)}}{\% \text{ Drug loading (theoretical)}} \times 100$$

1.5 *In vitro* drug release study:

On the basis of drug loading, particle size, SEM study and FESEM study, out of four formulations the F2 coded formulation was found to be the best on the basis of parameters investigated and considered for the further characterization.

About 2 mg of optimized formulation (F2) was weighed in three replicates and suspended in 2ml PBS (pH 7.4) ineppendorf tubes. After brief vortexing, the samples were incubated at 37˚C with constant shaking in an incubator shaker.Samples were kept for specific period of time up to 792 hours. At particular time interval 2 ml sample from each eppendorf tube was taken out and analyzed by using uv-visible spectrophotometer at a wavelength 480 nm. The volume of eppendorf tube was maintained upto 2 ml by adding fresh PBS and kept for incubation.

1.6 Preparation of aptamer-conjugated nanoparticle:

Prepared nanoparticles were suspended in sterile water (0.5 mg/ml). 300mM equivalent of EDC (1-Ethyl-3-(3-dimethylaminopropyl)carbodiimide) and 200mM equivalent of NHS (N-hydroxysuccinimide) were added to the mixture and it was gently stirred for20 minutes for activation of the carboxyl terminals of the PLGA. Aptamers with NH_2modification was dissolved in DNase RNase free water (5 µg/ml) and it was denatured and renaturedby heating to 90˚C for 10 minutes and snap frozen on ice. The aptamers were thenadded to the nanoparticles and they were allowed to react for 2 hours under gentle stirring.The product was then washed 4 times with DNase - RNase free water by multiplecentrifugation under 26000 rcf and resuspension. The end product was then lyophilized and stored under refrigerator.

1.7 Determination of aptamers conjugation by Agarose Gel electrophoresis:

To determine the successful conjugation of the DNA aptamers to the nanoparticles, agarose gel electrophoresis was performed. The electrophoresis was run with a 1x Tris-Acetate EDTA buffer across a 2% agarose gel.

1.7.1 Preparation of 1X Tris Acetate EDTA Buffer:

4.84 g of Tris base and 1 mM equivalent of sodium EDTA were dissolved in 900 ml of double distilled water. To the above solution 1.14 ml of glacial acetic acid was added and the final volume was made to 1 ltr by adding double distilled water.

1.7.2 Preparation of Loading Buffer:

A 6x loading buffer was prepared by dissolving equal volumes of distilled water and glycerol with around 0.5 mg of bromophenol blue. The loading sample for electrophoresis was prepared by dissolving 20 µl of loading buffer and 5 µl of the sample.

1.7.3 Preparation of 2% agarose gel:

Agarose (DNA grade, low melting) (1.5 g) was added in 75 ml of TAE buffer and microwaved for 2 minutes till a boiling, clear solution of agarose was formed. After cooling for few minutes, 10 µl of ethidium bromide solution (10 mg/ml) was added to the solution. The agarose solution was then poured on a 10 cm x 10 cm casting tray, taped on all sides, and the gel comb was placed near one of the ends of the tray. Then it was allowed to cool for an hour at 4˚C.

1.7.4 Running gel electrophoresis:

The tray containing 2% agarose gel mixed with ethidium bromide as imaging agent was placed in the electrophoresis chamber and the TAE buffer was poured over it into the chamber so that the gel was submerged about 2 mm under the level of the buffer. The 3 comb wells in the gel were filled with samples containing 100 bp DNA ladder, free aptamers and aptamers-conjugated nanoparticles respectively. The gel was then run from negative to positive at 50 volt (around 2.5 volt/cm) for about 1-2 hours. After the marker dye had reached about 75% of the gel length the power was turned off and the tray was taken out of the chamber. The buffer was dried of the surface and the gel was scanned under uv light in a uv transluminiscent chamber.

Chapter - 7

Results

RESULTS

7.1 The UV absorption spectra of Doxorubicin

For the determination of maximum absorption spectrum of Doxorubicin, a dilute solution of Doxorubicin in DMSO and PBS were prepared and scanned between 190-600 nm under UV-Vis spectrometer Intech-295 (USA) with DMSO and PBS as the blank reference. The spectrum (Fig 7.1 a) showed distinct peaks at 258.5 nm and 480 nm in DMSO and a characteristic peak of Doxorubicin at 480 nm in PBS (Fig 7.1 b). The 480 nm peak was selected as the representative peak of doxorubicin for preparation of standard calibration curve.

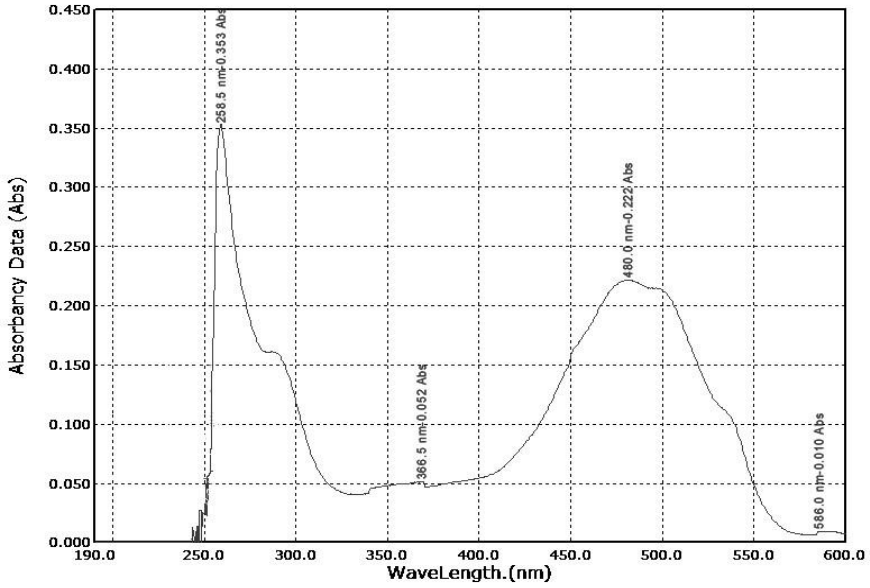

Fig 7.1 (a) The UV absorption spectrum of Doxorubicin in DMSO

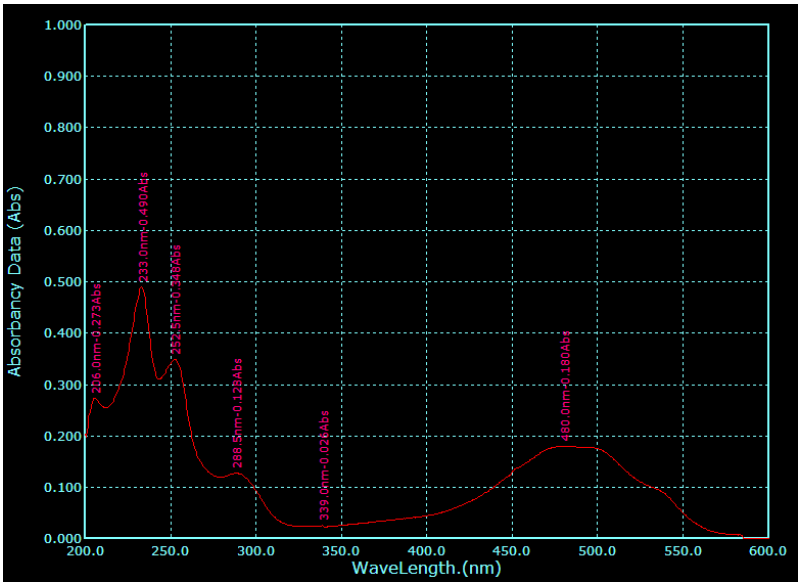

Fig 7.1 (b) The UV absorption spectrum of Doxorubicin in PBS

7.2 The calibration curves of Doxorubicin

Two different calibration curves of Doxorubicin were prepared- one in PBS (pH 7.4) for studying the *in vitro* drug release and another in DMSO for studying the drug loading of the nanoparticles. The dilutions prepared for calibration curve in DMSO were 1 µg/ml, 2 µg/ml, 4 µg/ml, 5 µg/ml, 6 µg/ml, 8 µg/ml and 10 µg/ml and for PBS the dilutions were made as 1 µg/ml, 2 µg/ml, 4 µg/ml, 5 µg/ml, 8 µg/ml and 10 µg/ml. The calibration curves for Doxorubicin in DMSO and in PBS are depicted in Fig 7.2 and Fig 7.3 respectively. The corresponding absorbance data against concentration is given in Table 7.1 and Table 7.2. for DMSO and PBS respectively.

Table 7.1 The mean absorbance of Doxorubicin samples against their concentrations in DMSO

Concentration µg/ml	Mean absorbance
1	0.013435
2	0.029004
4	0.057148
5	0.072539
6	0.086281
7	0.099725
8	0.114514
10	0.145409

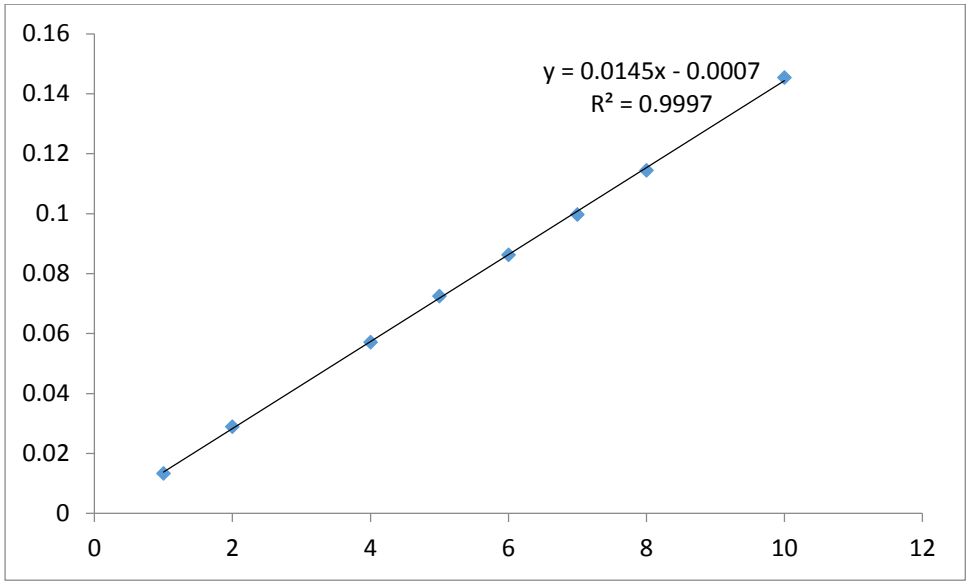

Fig 7.2 Calibration curve of Doxorubicin in DMSO

Table 7.2 The mean absorbance of Doxorubicin samples against their concentrations in PBS (pH 7.4)

Concentration µg/ml	Mean absorbance
1	0.001815
2	0.001672
4	0.005409
5	0.003488
8	0.009368
10	0.012514

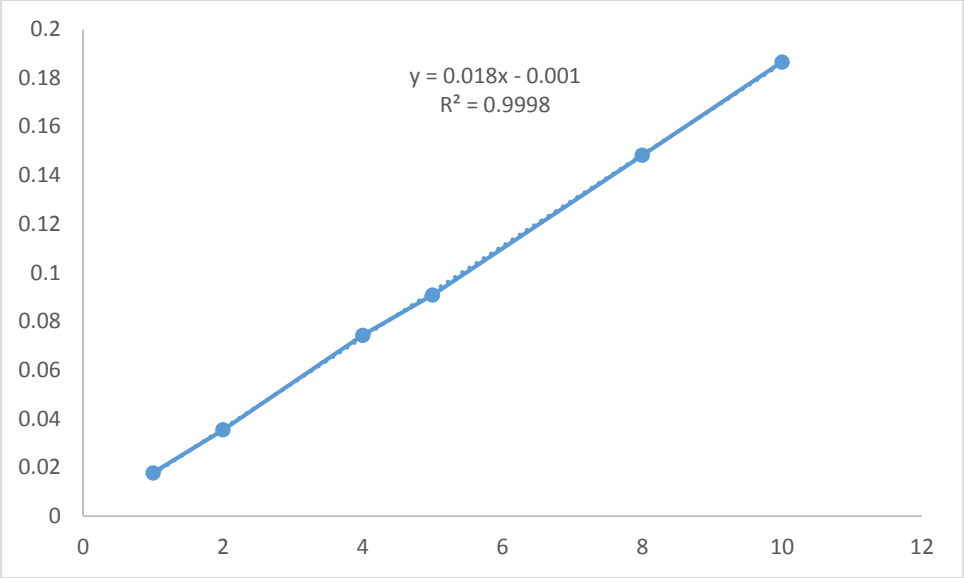

Fig 7.3 Calibration curve of Doxorubicin in PBS

7.3 The drug-excipient interaction study with FTIR spectroscopy

The FTIR spectra of Doxorubicin, PLGA, PVA, formulation and physical mixture have been given in Figures 7.3 (a - e) separately. Doxorubicin possesses different reactive functional groups such as NH_2, OH, H and C=O groups in its structure. In the FTIR spectrum of the drug, the peak which appeared at wavenumber 3330.25 cm^{-1} represents the stretching vibration of OH group, which lies between the wavenumber ranges from 3200-3500 cm^{-1}. The peak at 2930.83 cm^{-1} which lies between the wavenumber 2850-3000 cm^{-1} represents the presence of CH stretching vibration in the drug. The wavenumber ranges from 1665-1760 cm^{-1} indicates the presence of C=O stretching (general carbonyl) which supports the peak observed at 1729.44 cm^{-1}in the FTIR spectrum of the drug. In the spectrum of PLGA, the peaks observed in the wavenumber ranges from 2850-3000 cm^{-1}, are for the stretching vibration of CH_2, CH groups presents in the PLGA. The peak at wavenumber 3445.79 cm^{-1} in the PLGA spectrum belongs to the range 3200-3550 cm^{-1} for OH (H-bonded) stretching. The spectrum of PLGA (50:50 acid terminated) shows intense peak for COOH group at 1759.79 cm^{-1} that belongs to the wavenumber ranges from 1690-1760 cm^{-1} for carboxylic acid and derivatives. The peak in the spectrum of PLGA at 1091.92 cm^{-1} belongs to the range 1000-1320 cm^{-1} which represents the presence of CO group with stretching vibration. In the FTIR spectrum of PVA the broad peak at 3423.03 cm^{-1} is attributed for OH (H-bonded) stretching

vibration for functional OH group of PVA. The peak observed at 2938.41 cm^{-1} represents the presence of CH stretching vibration (alkanes) which ranges from 2850-3000 cm^{-1}.

All the characteristic peaks of PLGA, PVA and Doxorubicin appeared in the FTIR spectra of their physical mixture and the formulation. In the both spectra of formulation and physical mixture, the peak for PVA appeared at 3423.95 cm^{-1}, for PLGA at 1739.99 cm^{-1} and 1091.04cm^{-1}, for Doxorubicin at 1629.14 and 1273.38 cm^{-1}. However, there are some minor shifting of peaks that could be due to the physical interactions between drug and excipients.

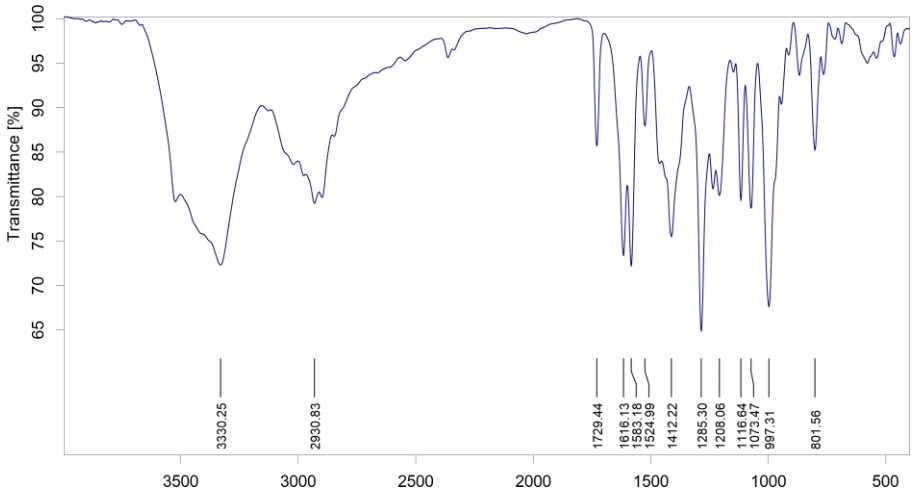

Fig 7.3 (a) FTIR spectrum of Doxorubicin

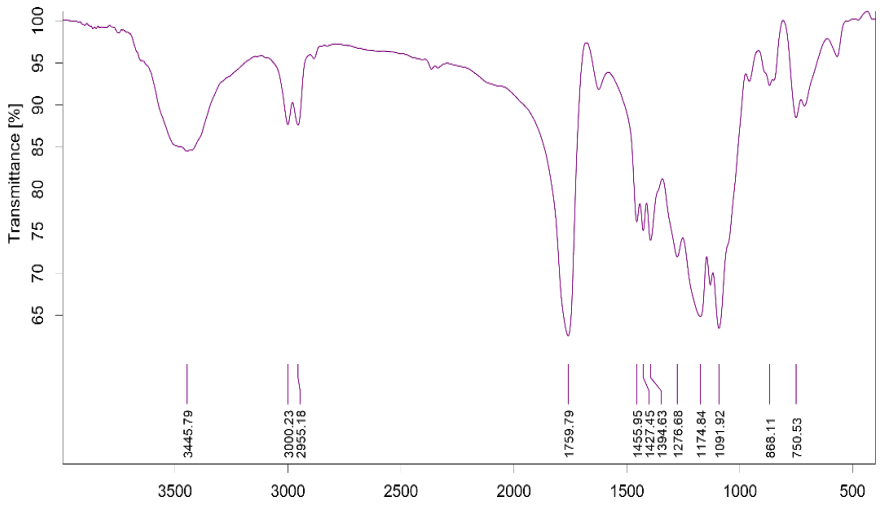

Fig 7.3 (b) FTIR spectrum of PLGA

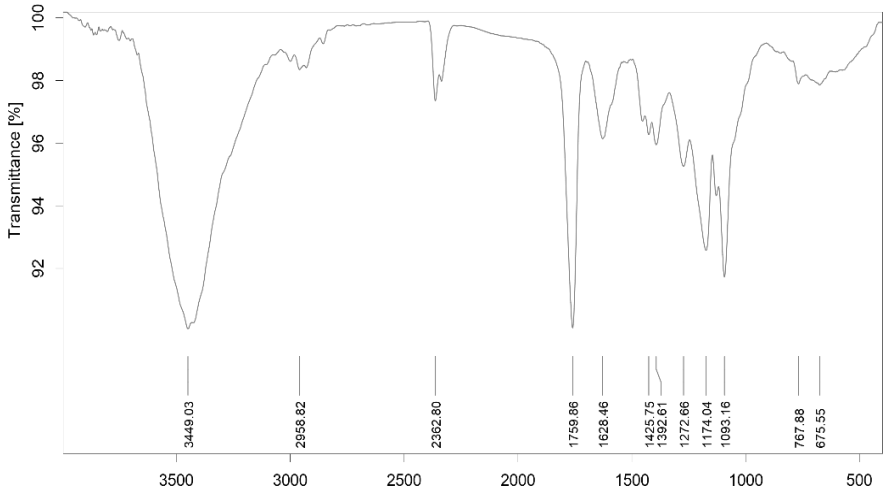

Fig 7.3 (c) FTIR spectrum of nanoparticle formulation

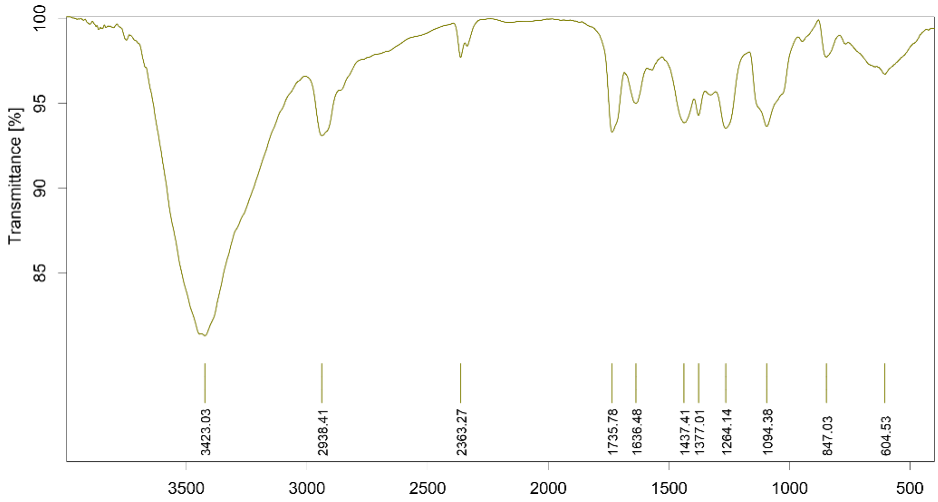

Fig 7.3 (d) FTIR spectrum of PVA

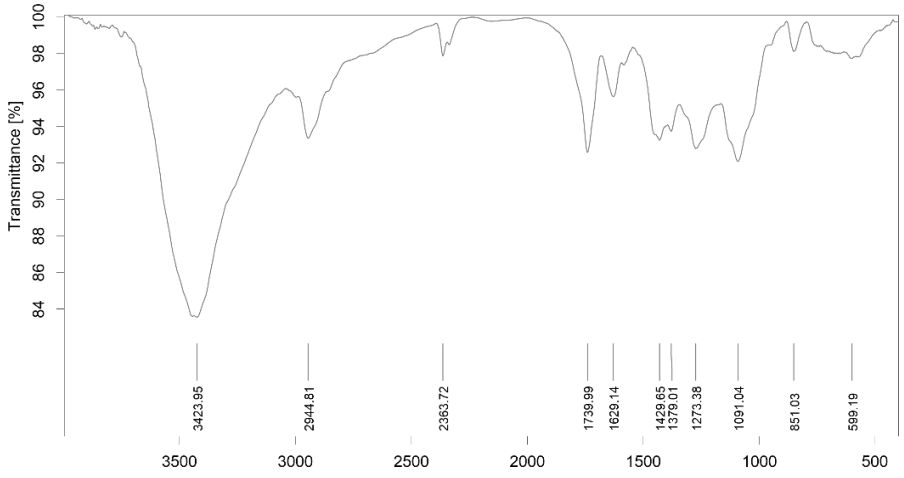

Fig 7.3 (e) FTIR spectrum of physical mixture

7.4 Study of morphology of nanoparticles by Scanning Electron Microscope (SEM):

Figures 7.4 (a-d) represents the SEM photographs of the formulations F1, F2, F3 and F4 respectively. The particles of all the four formulations were found to be nanosized and spherical in shape. As per the visual observation, F1 had spherical particles of the range 400-600 nm, while F2 showed particles of 400 nm size. Most of the particles in formulations F3 and F4 were within the range of 600 nm.

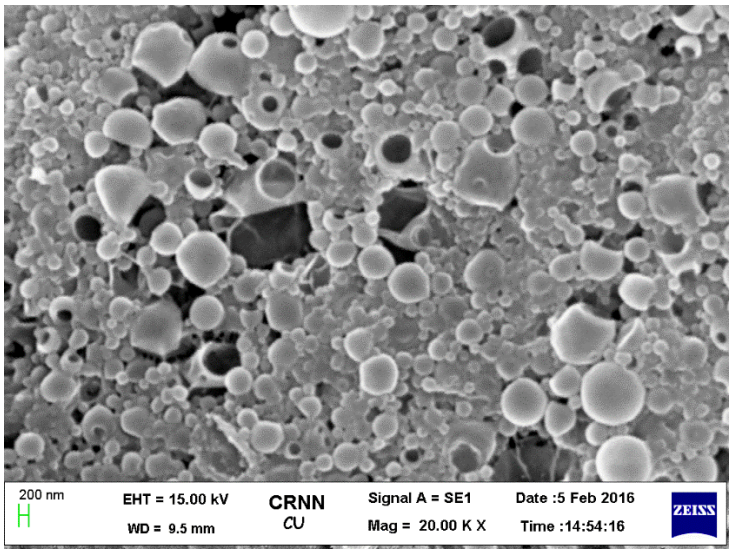

Fig 7.4 (a) SEM photograph of F1 nanoparticles

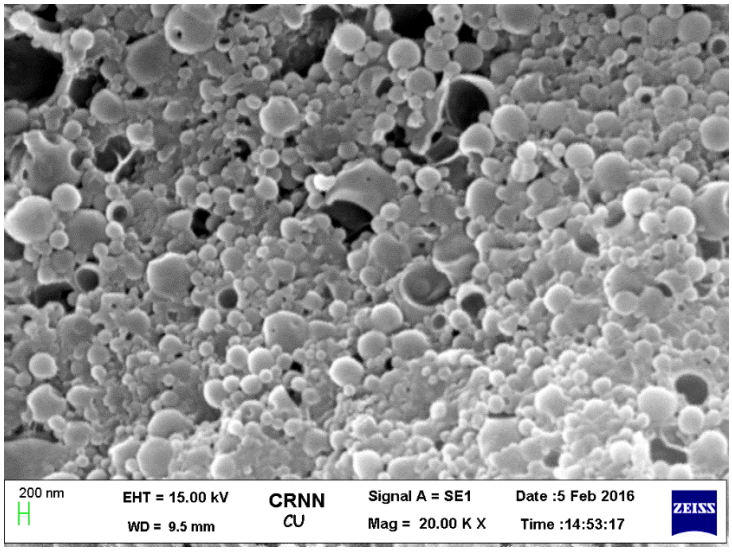

Fig 7.4 (b) SEM photograph of F2 nanoparticles

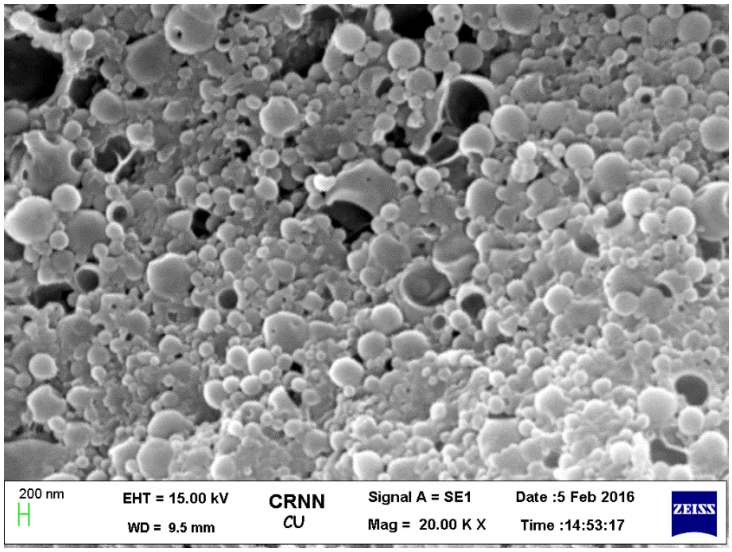

Fig 7.4 (c) SEM photograph of F3 nanoparticles

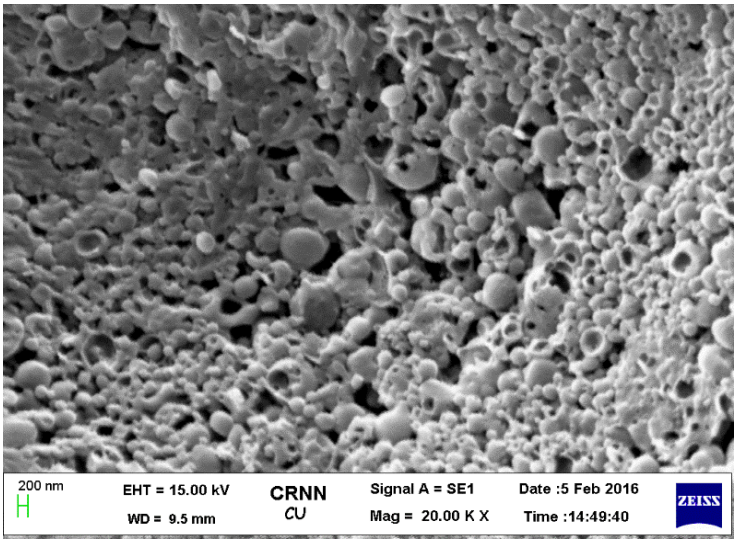

Fig 7.4 (d) SEM photograph of F4 nanoparticles

7.4 Study of morphology of nanoparticles by Field Emission Scanning Electron Microscope (FESEM):

On the basis of morphological characteristics as depicted by SEM study, two best formulations i.e. F2 and F4 were selected for FESEM study. Figure 7.5 (a - b) represents the FESEM photograph of formulation F2 and Figure 7.5 (c) represent formulation F4. Formulation F2 was found to be better than formulation F4, because it showed more uniform and spherical particles within 200-400 nm. Formulation F4 had particles between 300-600 nm, which is also nanosized but bigger in size than formulation F2.

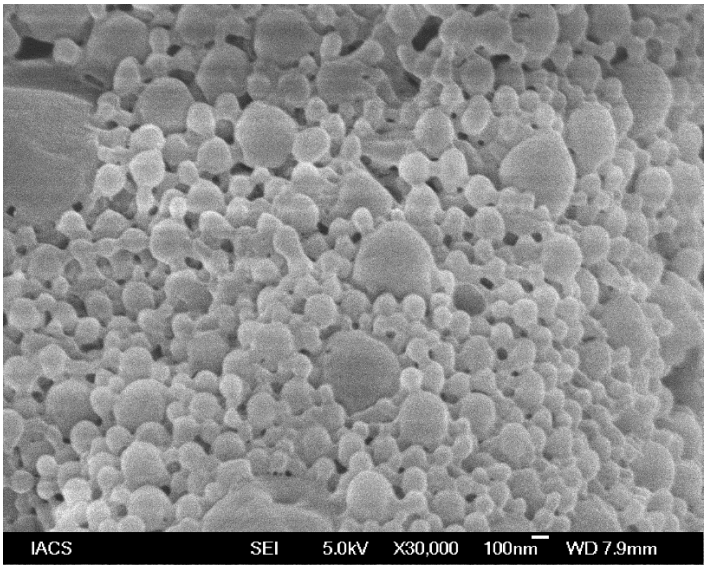

Fig 7.5 (a) FESEM photograph of F2 nanoparticles

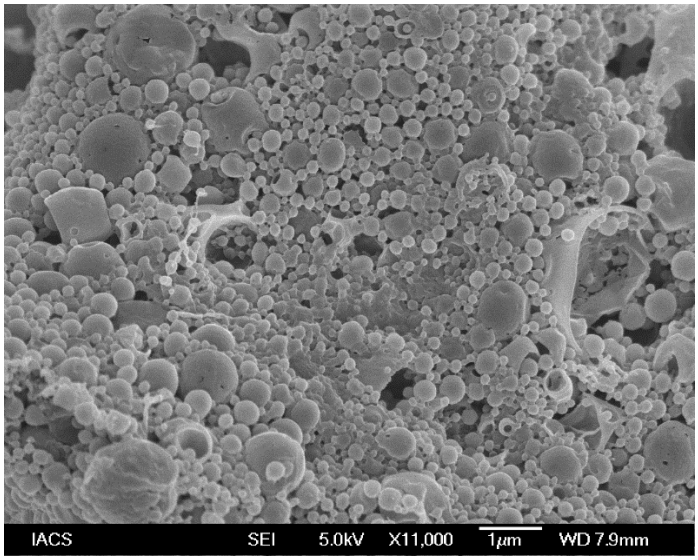

Fig 7.5 (b) FESEM photograph of F2 nanoparticles

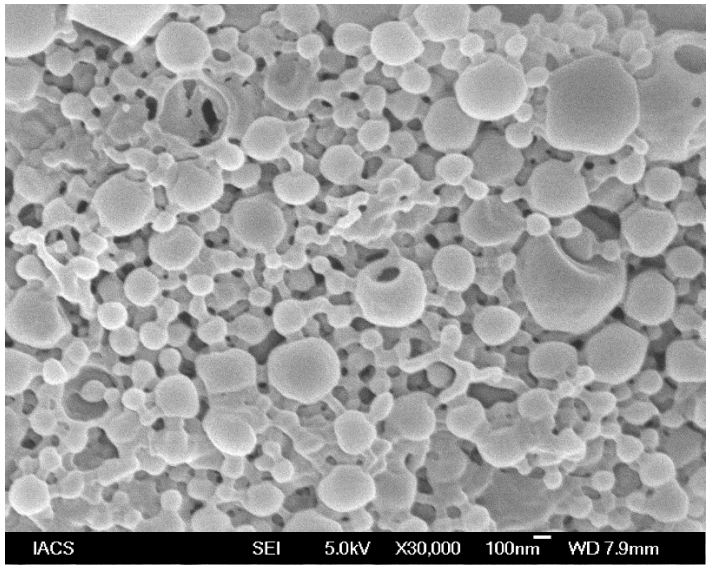

Fig 7.5 (c) FESEM photograph of F4 nanoparticles

7.5 Drug loading and Entrapment efficiency study:

Table 7.3 shows the practical and theoretical drug loading % along with entrapment efficiency of the formulations.

Table 7.3 Drug loading and % entrapment efficiency of the experimental formulations

Formulation	Amount of drug taken (mg)	Amount of PLGA taken (mg)	Conc. of inner and outer PVA solution (% w/v)	Theoretical drug loading (%)	Practical drug loading (%)	Entrapment Efficiency (%)
F1	5	50	2.0 and 1.0	8.74	3.75	42.90
F2	5	50	2.5 and 1.5	8.59	7.0	81.49
F3	5	50	3.0 and 1.5	8.23	4.0	48.60
F4	5	50	2.5 and 1.5	8.59	5.07	59.02

7.6 Size, Polydispersity Index and Zeta Potential of the particles:

Particle size distribution, polydispersity index (PDI) and zeta potential of the different formulations were measured by the instrument Zetasizer nano ZS (0.6 nm to 6000 nm) using DTS software V 4.0 (Malvern instrument Limited, Worcestshire, UK) which uses the principle of Dynamic Light Scattering. Table 7.4 gives the peak size, approximate peak intensity, standard deviation, mean size (Z average) and the polydispersity index of four formulations. Figures 7.6 (a), (b), (c) and (d) show the particle size distribution graphs of the formulations F1, F2, F3 & F4 respectively. The particles had average diameter varied from approximately 400 nm to 600 nm for F1 and F4 formulations. F2 had the lowest particle size of 361.1 nm as depicted in the figure 7.6 (b). The lowest polydispersity index was also obtained for F2 followed by F1 and F4. F3 showed an additional peak 10-100 nm range. This could be due to the cluster formation of some small particles.

Table 7.4

Formulation	Peak Size (nm)	Peak Intensity (%)	Z-Average Size (nm)	Standard Deviation	Polydispersity Index
F1	404.8	100	414.6	89.05	0.234
F2	376.7	100	361.1	72.41	0.045
F3	244.8	86.1	596.6	29.01	1.000
F4	423.9	100	532.5	77.02	0.316

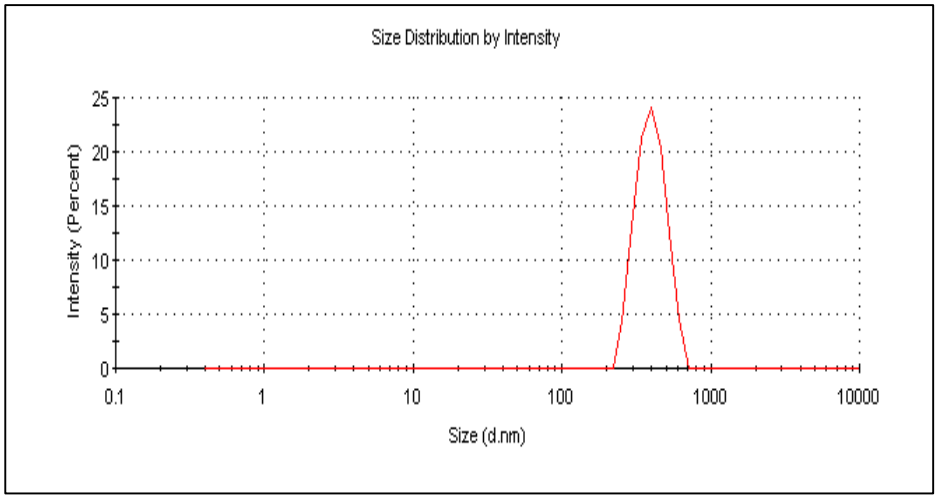

Fig 7.6 (a) Size distribution curve of F1

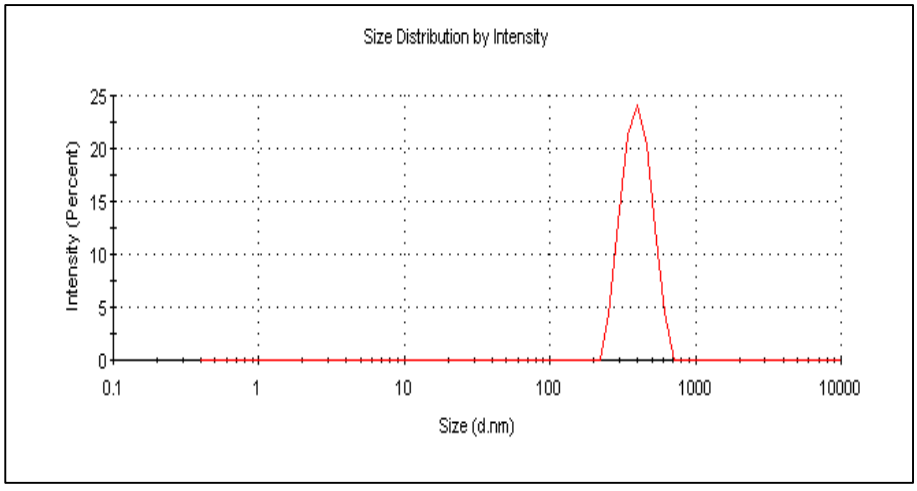

Fig 7.6 (b) Size distribution curve of F2

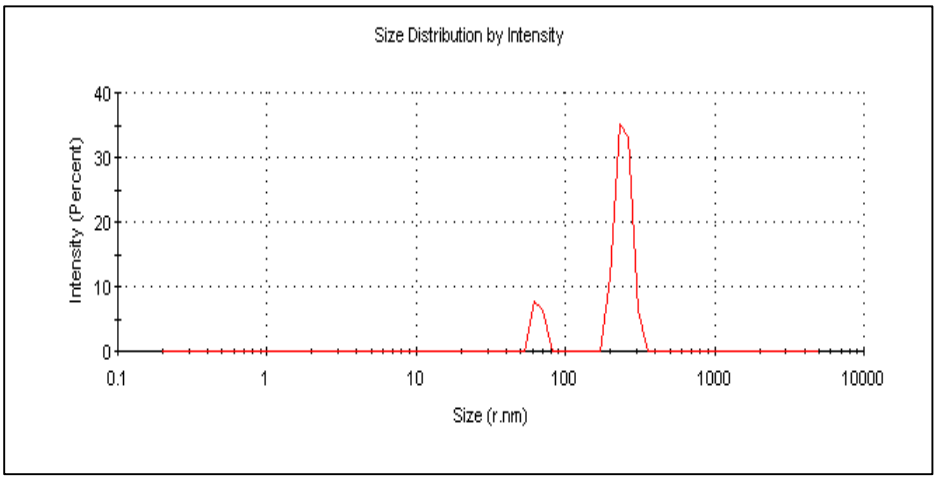

Fig 7.6 (c) Size distribution curve of F3

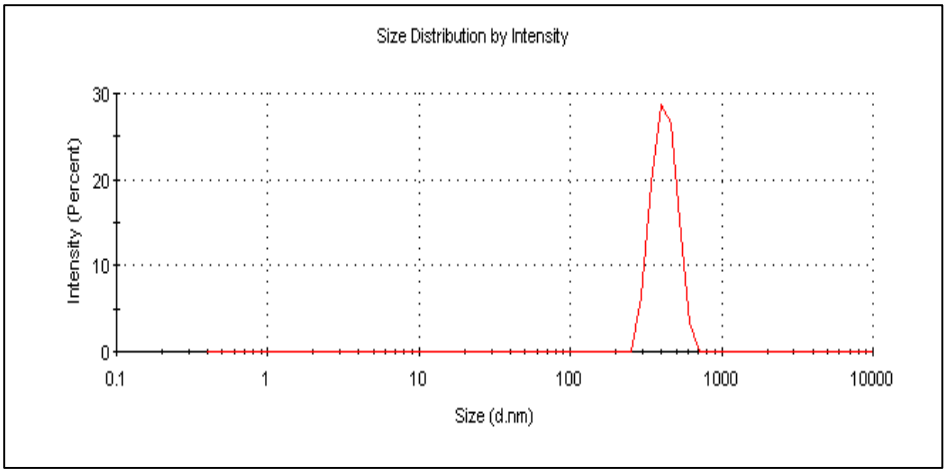

Fig 7.6 (d) Size distribution curve of F4

Table 7.5 shows the mean Zeta potentials, and the standard deviations of the four formulations. Figures 7.6 (e), (f), (g) and (h) show the zeta potential distribution graphs of the formulations F1, F2, F3 and F4. All the formulations had negative zeta potential values varied between -4.9 to -10.7 mV. This could be due to the presence of free carboxylic acid in the formulation.

Table 7.5

Formulation	Mean Zeta Potential (mV)	Standard Deviation
F1	-4.90	5.11
F2	-9.98	4.16
F3	-6.43	7.71
F4	-10.7	4.27

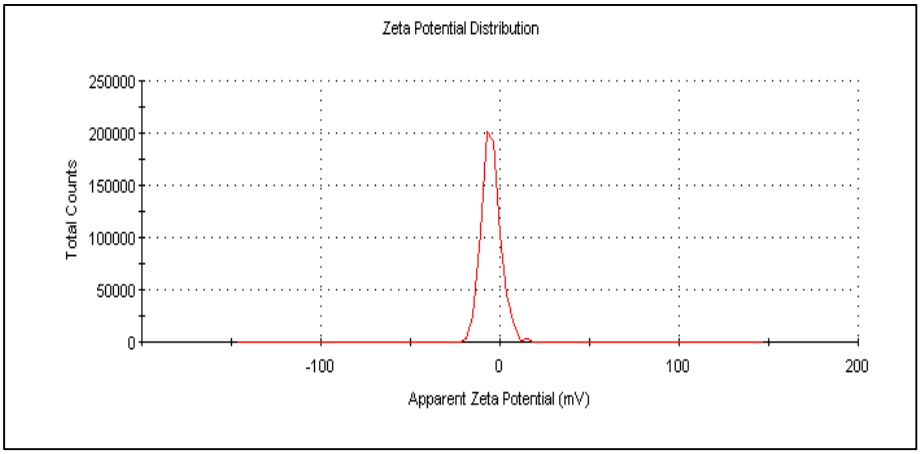

Fig 7.6 (e) Zeta potential of F1

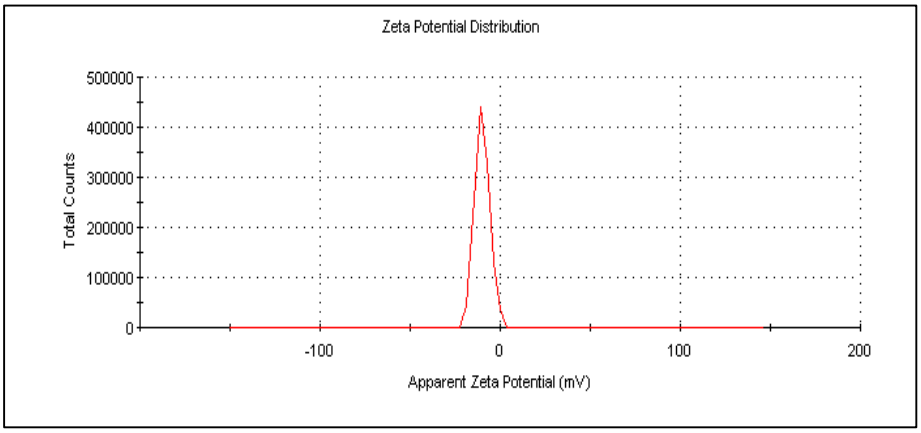

Fig 7.6 (f) Zeta potential of F2

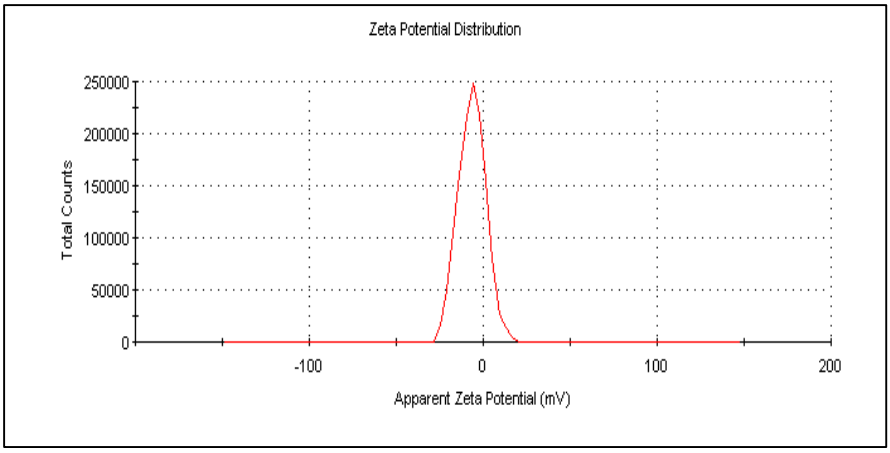

Fig 7.6 (g) Zeta potential of F3

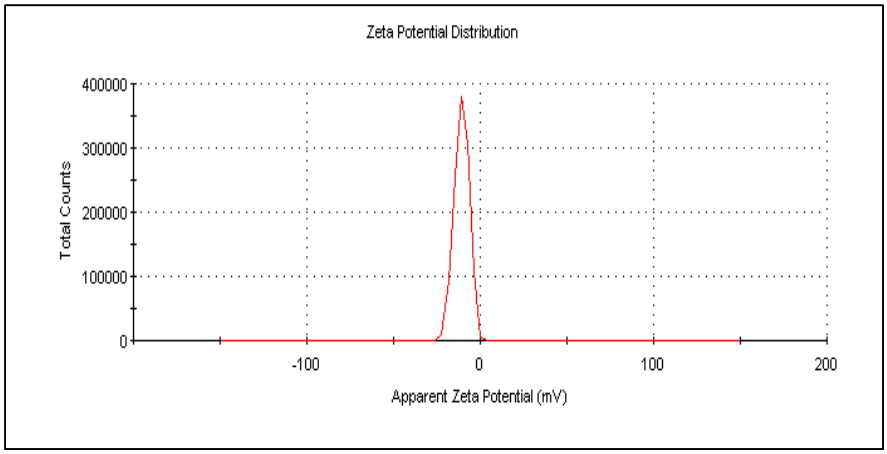

Fig 7.6 (h) Zeta potential of F4

7.7 Determination of conjugation of aptamers with the nanoparticles: 2% agarose gel was used to perform electrophoresis using 1x Tris-acetate-EDTA (TAE) pH 7.4 as running medium and ethidium bromide as the imaging agent for the DNA. The lanes of the well comb contained a 100 bp ladder, free aptamers (70 bp) and aptamer conjugated nanoparticles respectively. After running the gel for 2.5-3 hours, the gel slab was scanned under UV transluminiscent chamber.

It was observed that aptamer conjugated nanoparticles remained in the well as nanoparticles could not undergo electrophoretic movement. On the other hand, free aptamers showed band at 73 bp, showing the conjugation of aptamer with the formulation (Fig 7.7).

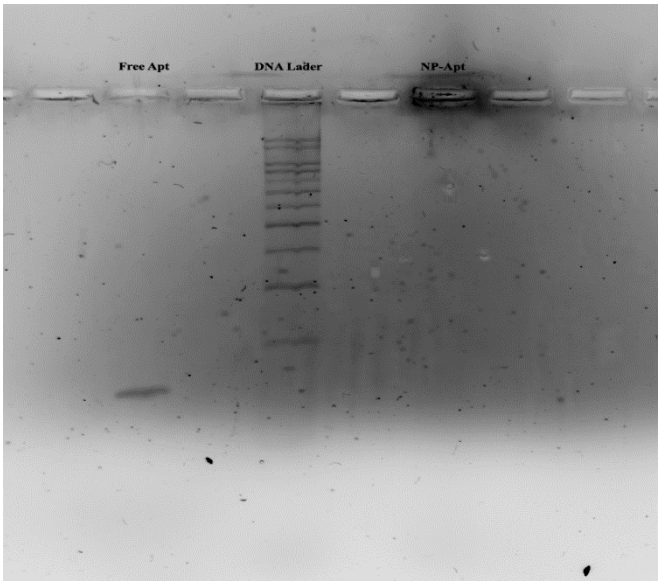

Fig 7.7 The Agarose gel electrophoresis process

7.8 In vitro drug release study:

On the basis of SEM and FESEM characteristics, particle size, drug loading and entrapment efficiency etc, formulation F2 was found to be the optimized nanoparticles formulation. So, this optimized formulation (F2) was selected for conjugation with aptamers and for *in vitro* drug release study.

Fig 7.8 (a) shows the release curve of the optimized formulation against time. Fig 7.8 (b) – Fig 7.8 (e) shows the *in vitro* drug release profile of the optimized formulation in different release kinetic model for 792 hours. Table 7.6 depicts the regression of data points from the best fit line, using different release kinetic models.

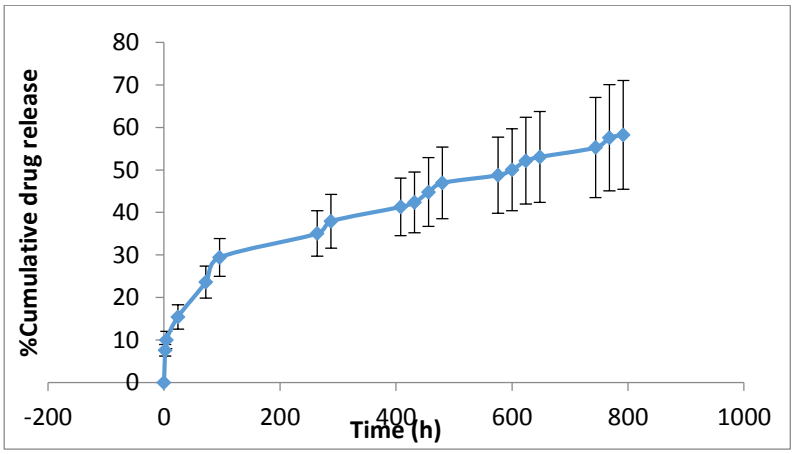

Fig 7.8 (a) Cumulative Release % of the drug from F2 against time

(1) Zero order kinetics:

In this kinetic model, cumulative amounts of drug released was plotted against time to find out the linearity with best fit line.

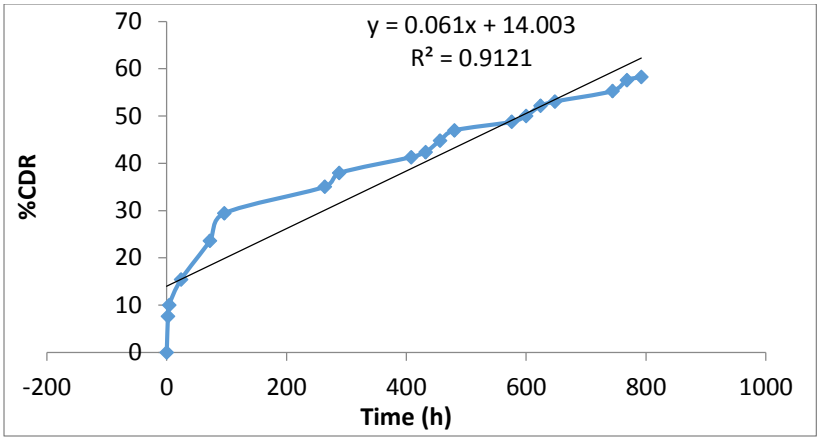

Fig 7.8 (b) The best fit lines with the cumulative drug release against time (Zero order)

(2) First Order Kinetics:

In this model, log % of ADR (amount of drug remaining to release) *versus* time was plotted.

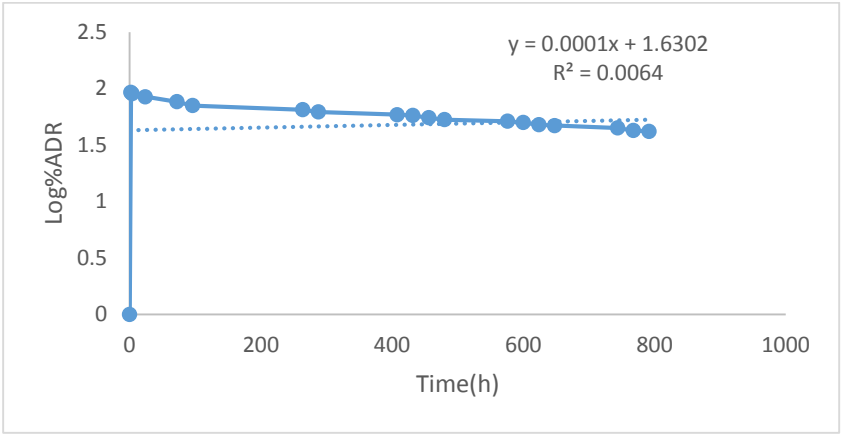

Fig 7.8 (c) The best fit lines to the log cumulative percentage of drug remaining *versus* time. (First Order)

(3) Higuchi Model:

The data obtained were plotted as cumulative percentage drug release versus square root of time and tested for best fit line.

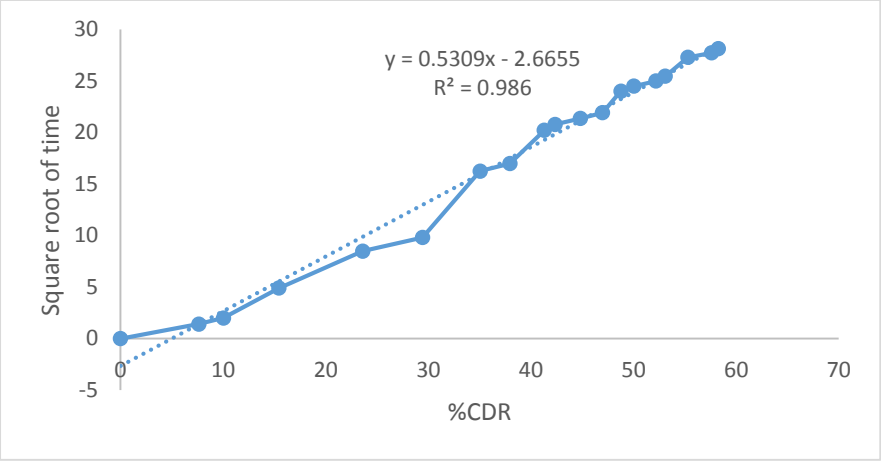

Fig 7.8 (d) The best fit lines to the cumulative release % against square root of time. (Higuchi)

(4) Hixson-Crowell Model:

Drug release data were plotted as cube root of drug percentage remaining in formulation *versus* time.

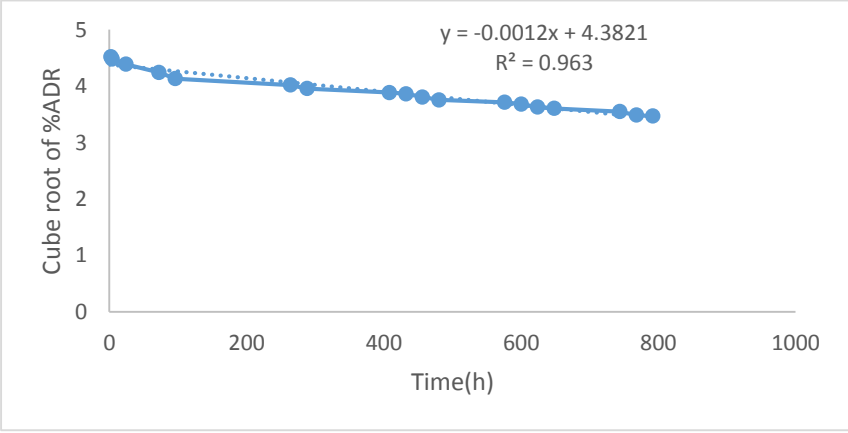

Fig 7.8 (e) The best fit lines to the cube root of percentage of drug remaining against time. (Hixson-Crowell)

(5) Korsmeyer-Peppas Model:

The data obtained from *in vitro* drug release studies were plotted as log cumulative percentage drug release *versus* log time.

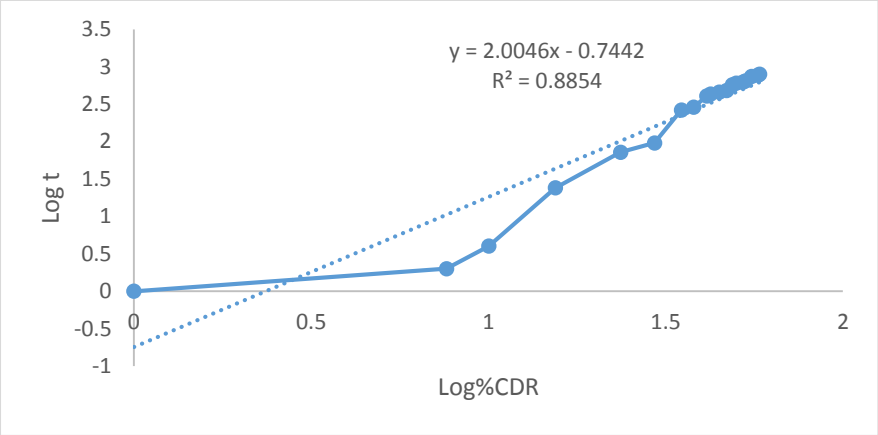

Fig 7.8 (f) The best fit lines to the log cumulative release % against log time. (Korsmeyer- Peppas)

Table 7.6 The regression values of the optimized formulation F2 by using different release kinetic models

	Zero Order	First Order	Higuchi	Hixson-Crowell	Korsmeyer-Peppas
R^2	0.9121	0.0064	0.986	0.963	0.8854

Chapter - 8

DISCUSSIONS

8.1 The UV absorption spectra of Doxorubicin in DMSO and PBS:

Doxorubicin was dissolved in DMSO and PBS separately and after scanning under UV spectrophotometer, the absorption maxima (λmax) was found to be 261nm and 480 nm (Fig 7.1 a) in DMSO and 480 nm in PBS (Fig 7.1 b). The absorption maxima (480 nm) was found to be common in both the mediums, which is one of the reported peak for doxorubicin [1]. This proves the purity of the product and provides the reference wavelength for the further spectrophotometric studies.

8.2 The calibration curves of Doxorubicin in PBS (pH 7.4) and DMSO:

Two calibration curves were prepared- one in PBS (pH 7.4) for studying the *in vitro* drug release and another in DMSO for studying the drug loading of the nanoparticles. In the developed calibration curve (Fig 7.2 and Fig 7.3), the values of R^2 were 0.9997 and 0.9998 respectively. The values favour the accuracy of the calibration curves used for further analysis.

8.3 The drug-excipient interaction study with FTIR spectroscopy:

The characteristic peaks of PLGA, PVA and Doxorubicin were present in the spectrum of their formulation and physical mixture. However the presence of some minor shifting could be attributed due to the physical interaction between the drug and excipients. Formation of weak hydrogen bond, interaction due to van der Waals force or dipole-dipole interaction among those functional groups might be responsible for the physical interactions [2]. The presence of all the characteristic peaks of the drug and the excipients suggests that there was no chemical interaction.

8.4 Study of morphology of nanoparticles by Scanning Electron Microscope (SEM):

Fig 7.4 (a-d) showed that the particles were nanosized and spherical in shape. The formulation F1 (Fig 7.4 a) showed spherical particles of the range 400-600 nm as observed visually, but there seems some agglomeration. The formulation F2 (Fig 7.4 b) contained slightly higher amount of PVA. Most of the particles in F2 had spherical and distinct particles with more uniformity of sizes than the other formulations and most particles were below 400 nm. Most of the particles in formulations F3 (Fig 7.4 c) and F4 (Fig 7.4 d) were within the range of 600 nm. Out of four

formulations, F2 represents the more uniform, spherical and distinct nanosized particles as seen visually.

8.5 Study of morphology of nanoparticles by FESEM:

Out of the four formulations, F2 and F4 were selected for FESEM study, because as per SEM study they were found to be better than other two formulations. In FESEM image, formulation F2 Fig 7.5 (a) and 7.5 (b) clearly represents uniform, distinct spherical particles within 200-400 nm as estimated visually, which also supports the SEM data of that formulation. However, formulation F4 (Fig 7.5 c) appears as 300-600 nm spherical particles which is also a nanosize range but are bigger in size than F2. So on the basis of SEM and FESEM images, we can conclude that the formulation F2 has been found to be the best in terms of size and shape of the nanoparticle formulations.

8.6 Drug loading & Entrapment Efficiency:

The drug loading and entrapment efficiency varied with the changes made in different formulations. Among the four selected formulations F1 had the lowest drug loading (3.75%) and entrapment efficiency (42.90%), while F2 had the highest drug loading (7.0%) and entrapment efficiency (81.49%). Formulation F3 and F4 had the drug loading 4.0% and 5.07% and entrapment efficiency of 48.60% and 59.02% respectively. F1 was prepared with 2% w/v aqueous PVA solution and 1% w/v aqueous PVA solution for inner and outer phases respectively, while F2 had a higher PVA concentration (2.5% and 1.5%) in PBS (pH7.4). F3 had 3% and 1.5% PVA solution in water and F4 had the same PVA concentration of F2 but in slightly alkaline PBS (pH8.0) (Table 6.1). Doxorubicin is a highly hydrophilic compound and being a weak base its solubility decreases with increasing pH [3]. F1 created an aqueous medium with an environment suitable for the dissolution of Doxorubicin. This might cause a major amount of the drug to be hostile towards being entrapped in a hydrophobic scaffold like PLGA and remained soluble in the aqueous media. This may be the rationale behind the low entrapment of drug. Due to the higher PVA concentration, the viscosity of the medium in F2 increased which made w/o emulsion more stable, the drug remained entrapped within the polymer scaffold leading to the higher entrapment of the drug. In F3, the nature of the aqueous medium was water like in F1 but with slightly higher PVA concentration. Due to the highly hydrophilic nature of Dox, the drug loading and entrapment efficiency was more or less similar in F1 and F3. Formulation F4 uses the PBS technique but at

pH 8, which further decreases the aqueous solubility of the drug along with the phosphate salts. But higher pH values (>9) react unfavourably with Doxorubicin and hence, are not suitable because they may induce unwanted chemical interactions with the drug.

8.7 Size, Polydispersity Index and Zeta Potential of the particles:

As depicted from Table 7.4 and 7.5, the formulation F1 had average particle size (Z-average) 414.6 nm and polydispersity index 0.234. The peak particle sizes of the other three formulations F2, F3 and F4 were 376.7, 244.8 and 423.9 respectively. There were a wider variation of particle size range as shown by polydispersity (PDI: 0.045, 1.000 and 0.316 respectively) of the formulation systems. The mean zeta potential data for all the four formulations were -4.90, -9.98, -6.43, and -10.7 respectively for F1, F2, F3 and F4. For a particle system to be stable in liquid dispersion they need to have a zeta potential of atleast -30 mV or +30 mV with more stability on either sides of this range [4]. Systems with zeta potential below 10 mV or above -10 mV are susceptible to flocculation. Therefore the zeta potential of all the four formulations (Table 7.4 & 7.5) suggests that they should be reconstituted just before administration and hence they require to be stored in freeze-dried form.

8.8 Determination of conjugation of aptamers with the nanoparticles:

In the figure 7.7 we can see that the lane had free aptamer beyond 100 bp as the aptamer had a length of 73 bp. Lane containing aptamer conjugated nanoprticles had illumination only at the well which proves that the DNA aptamers (causing the illumination by ethidium bromide) have been chemically conjugated with the nanoparticles and so they did not migrate towards the positive electrode. This proves success of carbodiimide chemistry for conjugation of aptamers with the nanoparticles and supports the possibility of linking a wide range of lingands with the different type of nanoformulations.

8.9 In vitro drug release study:

In vitro drug release data were collected over 792 hours and the cumulative release of drug from the optimized formulation F2 was plotted against time to determine the drug release pattern (Fig

7.8(a)). From the figure it is seen that almost 60% of the initial drug content released in 792 hours. The graph clearly showed the sustained release profile of the drug from the formulation.

The drug release pattern was also correlated with the established models of release kinetics namely Zero Order, First Order, Higuchi, Hixson-Crowell and Korsmeyer-Peppas. Considering the R^2 values (0.9121, 0.0064, 0.986, 0.963, 0.8854 respectively) in all the above mentioned kinetics model, it has been found that the drug release pattern followed Higuchi model (R^2 0.986) more than the other kinetics model. Higuchi model describes drug release patterns from matrix-like systems and indicates the release of drug mostly through diffusion and the erosion of the matrix polymer and may play some role to the formation of pore like systems [5].

REFERENCES

1. Rudra A., Manasadeepa R., Ghosh M.K., Ghosh S., Mukherjee B., 2010. Doxorubicin-loaded phosphatidylethanolamine-conjugated nanoliposomes: in vitro characterization and their accumulation in liver, kidneys, and lungs in rats. Int J Nanomedicine, 5, 811–823.
2. Maji, R., Dey, N.S., Satapathy, B.S., Mukherjee, B., Mondal, S., 2014. Preparation and characterization of Tamoxifen citrate loaded nanoparticles for breast cancer therapy. Int J Nanomedicine, 9, 3107-3118.
3. Wohlfart, S., Khalansky, A.S., Gelperina, S., Maksimenko, O., Bernreuther, C., et al. 2011. Efficient Chemotherapy of Rat Glioblastoma Using Doxorubicin-Loaded PLGA Nanoparticles with Different Stabilizers. PLoS ONE 6(5): e19121.
4. Yue, P.F., Yuan, H.L., Yabg, M., 2008. Preparation, characterization and pharmacokinetic evaluation of puerarin submicron emulsion. PDA J PharmSci Technol. 62, 32–45.
5. Costa, L., Lobo, J.M.S., 2001. Modeling and comparison of dissolution profiles. Eur. J. Pharm. Sci. 13, 123–133.

Chapter - 9

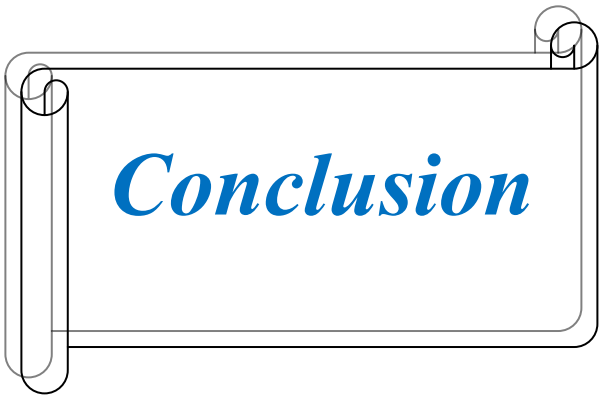

CONCLUSION

The present study developed a biodegradable and biocompatible polymer-based nanoparticulate drug delivery system. Doxorubicin-PLGA nanoparticles were developed using multiple emulsion-solvent evaporation technique. The optimized formulation (F2) was found to be within nano size range, spherical in shape and had smooth surface as depicted by SEM and FESEM. The drug loading was found to be around 7% with a sustained drug release profile over an extended period of time of 792 hours. Further, the optimized nanoparticle formulation was selected for the conjugation with aptamers using EDC/NHS technique. The conjugation was confirmed by agarose gel electrophoresis. The attachment of aptamers ligand increases the specificity of these nanoformulations to a particular phenotype of cancer cells and hence this approach in future would result in smart medicines which can be able to distinguish between the healthy cells and cancerous cells and show their cytotoxic activity likewise. Further studies including *in vitro* cytotoxicity assay, FACS and Confocal imaging need to be done to assure the specificity of the ligand attached nanoparticles over the non-conjugated ones. Also *in vivo* antitumor activity can be done so as to test the hypothesis of aptamers efficacy in a biological system.